SUBMITTED VERSION - ADDITIVE MANUFACTURING

Review Article

See the final published version at
https://doi.org/10.1016/j.addma.2022.103335

Overview of Debinding Methods For Parts Manufactured Using Powder Material Extrusion

Zahra Lotfizarei[1], Amir Mostafapour[1], Ahmed Barari[2], Alireza Jalili[1], and Albert E. Patterson[3,4]*

[1] *Department of Mechanical Engineering, University of Tabriz, Tabriz, Iran*
[2] *Faculty of Engineering and Applied Science, Ontario Tech University, Oshawa, Ontario, Canada*
[3] *Faculty of Manufacturing and Mechanical Engineering Technology, Department of Engineering Technology and Industrial Distribution, Texas A&M University, College Station, TX 77843*
[4] *J. Mike Walker '66 Department of Mechanical Engineering, Texas A&M University, College Station, TX 77843*

* *Correspondence:* aepatterson5@tamu.edu

Abstract

Material extrusion additive manufacturing (MEAM) is a common family of additive manufacturing processes based on the selective extrusion of a molten material in layers to build solid geometry. One of the emerging processes within this group is powder material extrusion (PME); in theory, it is based on the very common material extrusion (per ISO/ASTM 52900) process but uses modified hardware and design approaches to extrude feedstock consisting of metal or ceramic powder suspended within a thermoplastic matrix. The percentage of powder can vary from around 50% up to over 90%, making PME a feasible alternative to powder injection molding (PIM), some powder bed fusion (PBF) additive processes, and some powder metallurgy (PM) processes due to its very low cost, simple processing equipment, lack of industrial hazards, and lack of residual stresses. The produced parts are green, similar to what is obtained when using PIM, some PBF, and PM, and require debinding and sintering in order to be useful in practice. Much remains in development about how to properly use and design PME parts, including filament making, process steps, binder selection, debinding method, sintering approach, and characterization of the final parts. In order to contribute to more widespread adoption of the PME process for metals and ceramics, a comprehensive review of the literature on debinding processes relevant to PME was completed and is reported in this article. This review presents the state-of-the-art, discussed some useful and relevant approaches for the future from other manufacturing processes, and shines light on the needed work in this area for the advancement of PME as an end-user manufacturing process. This work, combined with knowledge of the sintering process, will provide a guide for future research and implementation of PME.

Keywords: Powder material extrusion (PME), metal additive manufacturing, ceramic additive manufacturing, debinding and sintering, feedstock, powder-based manufacturing

Nomenclature

AM	Additive manufacturing
Brown	Part after debinding and before sintering
Green	Raw part before debinding

PIM Powder injection molding

PM Powder metallurgy

PME Powder material extrusion (used with metal, ceramic, and mixed powder)

1. Introduction

Powder material extrusion (PME) (Figure 1) is one of the processes within the material extrusion (as defined by ISO/ASTM 52900) additive manufacturing (MEAM) family. It is similar in principle to the standard MEAM process (often known as fused filament fabrication (FFF) or fused deposition modeling (FDM) in practice), but uses modified hardware such as wear-resistant handling parts, larger-diameter steel extrusion dies, and pre-heating devices for the filament to allow it to use very abrasive and brittle (Figure 2a) input filament. The raw material for PME consists of a thermoplastic matrix with powdered metal, ceramic, or mixed metal/ceramic material embedded [1–11]. This powder-based extrusion process is known by several names in the literature, so for consistency and simplicity, it will be referred to as powder material extrusion (PME) throughout this article. Other variations exist which use a plunger or screw to extrude the material [1, 12], but these are rarely used. In order to bind the scope of this article and allow more depth of analysis, only filament-based processing were considered to be part of the core review. Texts discussing other AM-based processes and traditional powder processes were included as references to demonstrate the presented concepts.

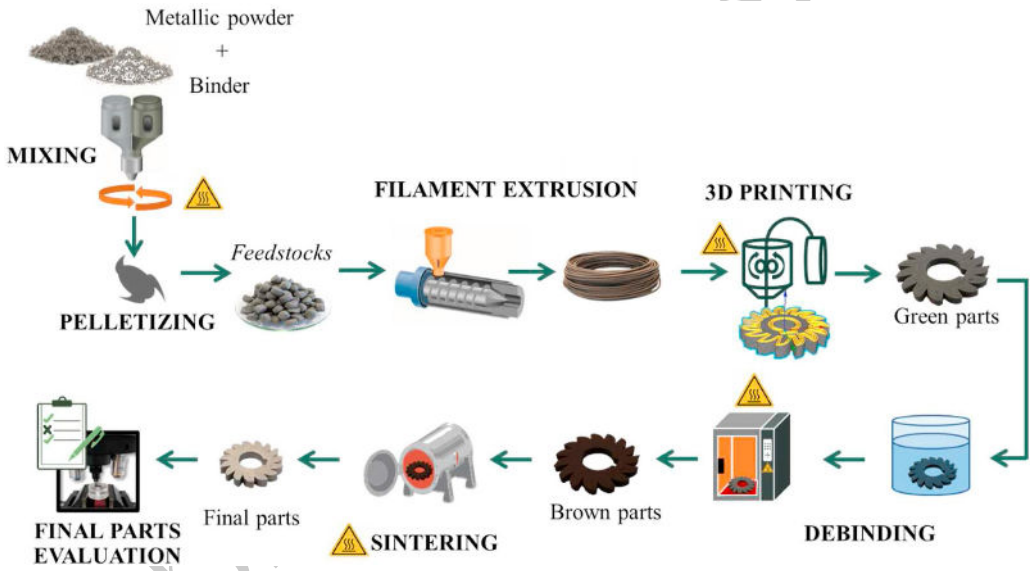

Figure 1: PME workflow from basic ingredients to final part evaluation [13]. Figure reproduced under the terms of a CC-BY license.

While metal- or ceramic-infused feedstocks have long been available for traditional MEAM, the amount of powder embedded in the filament is usually very low (typically 5-10%) and its benefit is primarily cosmetic [14–16]. The filaments used for PME is generally at least 50% powder and can be over 90% (for example, the filaments and pellets available from The Virtual Foundry [17], BASF [18], and other sources [6, 19, 20]). Using this feedstock, PME can produce parts that rival those produced using powder injection molding (PIM), powder-bed fused additive processes such as selective laser sintering (SLS), and some powder metallurgy processes (PM). When used for an appropriate application, processing of green parts using PME can provide a significant reduction in cost, risk, and processing complexity, since the equipment used is relatively simple and low-cost, does not require specialized tooling, and the final parts lack significant residual stresses [1, 4–6, 8, 21–28]. Thus far in the literature, the vast majority of studies using PME have used stainless steel or titanium alloys as the powder; a sampling of the other major materials that have been successfully processed as green parts using PME are presented in Table 1; note that this is an illustrative but not exhaustive list. Figures 2b-d show examples of PME feedstock filament with copper, stainless steel, and bronze powder.

Table 1: Example successful green part printing studies using PME.

Powdered Material	Example Successful Studies
Stainless steel (all alloys)	[1, 7–10, 17, 28–38]
Titanium alloys	[3–5, 17, 39, 40]
Aluminum alloys	[17, 41, 42]
Copper alloys	[17, 43–45]
Nickel alloys	[17, 46]
Other iron-based alloys	[13]
Ceramics	[6, 47–54]

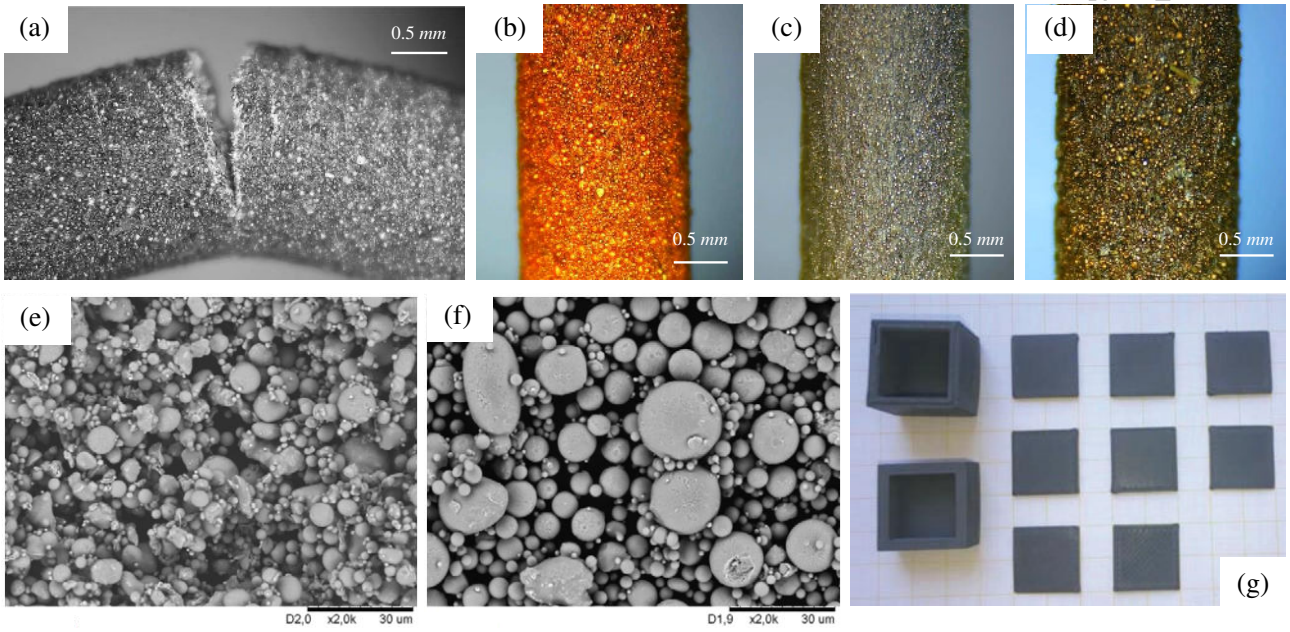

Figure 2: (a) Example of broken PME filament from gentle bending, (b) example copper PME filament (90.1% powder) with PLA binder, (c) example 316L stainless steel PME filament (85.2% powder) with PLA binder, (d) example bronze PME filament (88.9% powder) with PLA binder, (e-f) stainless steel powder used for successful PME printing [3], and (g) example printed green PME parts [3]. Figures (a)-(d) original to this article. Figures (e)-(g) from [3] and reproduced under CC-BY license terms. The materials shown in panels (a)-(d) manufactured by The Virtual Foundry [17].

While the PME process is conceptually simple, a number of important considerations need to be made before using the process to create end-user (i.e., ready for debinding and sintering) green parts. The most important of these is the quality of the input material; unlike PIM and PM, the thermoplastic matrix and powder mixing must be done well in advance of the processing and the filament printed without further mixing or kneading (such as would be done by an injection screw in PIM). Therefore, the quality of the feedstock filament (for both PME and PIM) has a major impact on the quality of final part. Some of the areas where problems can occur include in the ratio of matrix/binder material and powder, the homogeneity of the mixture, the quality of the raw materials, and the size and consistency of the powder particles. The feedstock also needs to be handled and stored correctly before use, as even high-quality material can be damaged and degrade due to bending, stretching, and material creep at elevated temperatures and high humidity; this is especially an issue for materials where the binder has a low glass transition temperature, as some can begin to creep and structurally degrade at temperatures as low as 60°C [16, 33, 55–57]. PME filament (the same as for PIM feedstock) is also generally quite brittle, given the high percentage of powder, necessitating even more care to avoid breakage and cracks in the feedstock. Final parts made from damaged or degraded filament may have poor layer binding, sinks and cavities, poor surface finish, and internal voids even after debinding and sintering [7, 16, 21, 22, 24, 33, 58, 59]. Due to the nature of extrusion-based AM, internal defects in the part may not be detected until long after the printing and even

after the part has been put in service.

Table 2: Example powder size and shape [60]

Powdered Material	Powder Particle Shape	Average Particle Size (μm)
Yttria stabilized zirconia (YSZ)	Irregular	0.6
Stainless steel (316L)	Spherical	8.6
Stainless steel (17-4PH)	Spherical	12.3
Titanium alloy (Ti6Al4V)	Spherical	14.97

When using PME, it is assumed that the MEAM-related parameters (print temperature and speed, layer adhesion, and other considerations) are properly tuned for the material at hand and so the green parts should be good quality if the process is successful. From here, the successful debinding and sintering of the green parts depend on the relative shrinkage of the elements containing the powder, as well as the uniformity of the powder distribution throughout each element [31, 32, 61]. In addition to printing considerations, the quality of the powder is also a concern, as the powder particles are not necessarily uniform in shape and large particles can cause nozzle clogging. Particles with sharp edges can also cause stress concentrations within the green parts, potentially initializing a crack. Some of the work done by C. Kukla and collaborators [3, 21, 22, 29, 30, 58, 60–62] looked at the impact of powder size for PME; some results from successful prints are shown in Figure 2g and Table 2. The standard available extrusion nozzles for PME range from 0.4 mm to 1.0 mm in diameter, so the standard particle sizes shown in Table 2 should not interfere with printing.

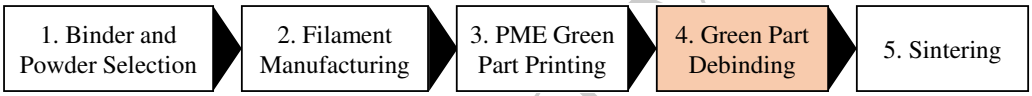

Figure 3: Major research areas for PME. This review focuses on (4) Green Part Debinding. Figure original to this article.

PME is a relatively new process that is very promising for manufacturing useful metal additive manufactured parts. It is complementary with existing processes such as metal injection molding (PIM) and powder metallurgy (PM). For it to be more widely used and implemented, research in five major areas is needed. Figure 3 shows the five topics, beginning with binder and powder selection and ending with the final sintering (and any needed post-processing) of the part. As shown in the literature discussed in this section, a significant amount of work has been done in all of the areas, particularly in the first three. While more work is needed, enough has been done to help guide useful application and design for the process. Relatively little has been done for debinding and sintering. Since the sintering process is likely to be the same or very similar as that used for PIM and PM, the focus of current research efforts should be the debinding. In order to establish the state-of-the-art and explore the available debinding methods which may be relevant to PME, the current article explores these methods and analyzes them for fitness and applicability to PME. It should be noted that not all of the explored literature is directly on PME, but all present methods that may be applied to it under various circumstances. A set of examples specifically for PME us presented for each of the major debinding methods.

This review is presented in sections, beginning with a description of the review approach and methodology (Section 2). This section includes details about the literature search and acceptance/exclusion criteria for included papers. Section 3 discusses the production and selection of feedstock for PME, which provides technical context for Section 4 on debinding processes. This is followed by a discussion on defects and process errors related to debinding in Section 5. Finally, recommendations for implementation and future work are given in Section 6 and Section 7.

2. Review Approach and Major Research Questions

This section provides a brief summary of the approach and selection method for the review presented in this article. To begin the review, a set of approximately 50 relevant keywords were compiled by the authors, which were then used to search for literature in Google Scholar, Scopus, ResearchGate, and the major AM, manufacturing, and powder processing journals and international conference proceedings. A general Google

search was completed as well to make sure no major relevant literature was missed. The reference lists of each found paper were examined as well, which led to the addition of several papers missed during the initial literature review. A set of unique papers was found, each of which were deemed relevant based on title and abstract. The full texts of these were then collected, reviewed, and scanned for general relevance and credibility. After careful screening and deep review, the final set of papers was decided on by the authors. Papers related to PME directly were prioritized, but papers related to general AM, traditional MEAM, metal injection molding, and powder metallurgy were also included if they fit within the scope of this article. Excluded from the final set of papers were papers not in English, conference papers with a published journal version (where the journal version was included in the final set), non-peer reviewed technical reports and lecture notes (with the exception of those from The Virtual Foundry and BASF, which are widely referenced in this field), and papers published in clearly predatory journals or unknown conferences. All the figures collected for the final version of the review were used under the terms of a CC-BY license or reproduced with written permission from the copyright holder (specifically Elsevier B.V. and John Wiley and Sons, Inc. for this article) per relevant copyright laws and publishing norms. The major research questions explored in this review were:

1. What debinding methods have been used directly for PME in the reviewed literature?
2. What debinding methods have been used for other powder-based manufacturing processes (PIM, PM, other AM processes) which are relevant or applicable for future uses with PME?
3. What are the basic mechanics of the reviewed debinding methods, including information about advantages and disadvantages and best practices?
4. Can the debinding methods reviewed be directly compared with each other, relative to their real or potential use for PME?
5. How does the feedstock manufacturing process (both for filament and for pellets) affect the outcome?
6. What special considerations need to be made during feedstock manufacturing for PME?
7. What are the major needed future research directions for debinding of PME parts?
8. Given the collected technical and use-case information from this review and their technical expertise, what future recommendations can be provided by the authors in this area?

3. Overview of Feedstock Production

The binder system used to produce feedstock ready for PME and other processes typically consists of one or more thermoplastic polymer components mixed together [3, 8, 21, 58, 63, 64]. The selection of binder components and the production technique are important, as this can have a large influence on the final sintered parts, even if completely removed during debinding [22]. In general, the binder components fall into three categories [20, 65]:

1. **Main binder** ($50-90\%$): The main ingredient of the binder system is the polymer that is present in the maximum amount and is first removed in the debinding stage. Generally, a material with low molecular weight is selected so the lower viscosity will prevent interference with the powder and heavier components.
2. **Backbone** (Up to 50%): The second component is the backbone (which does not react during the debinding process) that is utilized to hold together the brown part after debinding. The backbone is thermally degraded before or during sintering.
3. **Additives** (Up to 10%): Additives such as dispersant agents, compatibilizers, plasticizers, waxes, and stabilizers help the powder particles to disperse into the binder uniformly, preventing separation and agglomeration of the components.

The backbone is typically a thermoplastic polymer; the selected backbone polymer enormously influences not only the green processing of the feedstock in PME (and other processes) but also strongly influences the final mechanical properties and dimensional accuracy of the sintered part [8, 9, 20, 65]. Examples of common thermoplastics suitable for use as binders are shown in Table 3. Other specific ingredients of the binder systems are tackifiers, waxes, and plasticizers. For example, to promote the adhesion with the former layer and create flexibility in the filament in PME, and tackifier like hydrocarbon resin has been used [66]. On the other hand, waxes such as partial crystalline polyolefine, paraffin, monotan, and carnauba have been utilized to decrease viscosity and improve the stiffness of feedstock [8, 54, 67–69]. These materials not only promote flowability (important in both PME and powder molding processes) but also should be easily eliminated in the processing. These polymers also supply particle lubrication, improve tool life, promote particle packaging,

Table 3: Common thermoplastic materials that are suitable for use as binders with the abbreviations used in this review and discussion. The types of binders stated here were taken from the various papers reviewed for this article and cited in the reference list.

Thermoplastic	Abbreviation
Acrylonitrile butadiene styrene	ABS
Dioctyl phthalate	DOP
Dibutyl phthalate	DBP
Polyolefin	PO
Polyethylenes (high/low density)	HDPE/LDPE
Polyethylene wax	PEW
Polypropylene	PP
Polymethyl methacrylate	PMMA
Ethylene vinyl acetate	EVA
Polyoxymethylene or polyacetal	POM
Polyethylene glycol	PEG
Ethylene acrylic acid	EAA
Stearic acid	SA
Nylon	PA
Polylactic acid	PLA
Thermoplastic elastomer (thermoplastic rubber)	TPE
Paraffin wax	PW
Styrene ethylene/butylene-ethylene copolymer	SEBS

improve flow, and often boost the strength of the powder formed in the green part [70]. Careful manufacturing of the feedstock helps to maximize the homogeneous distribution of powder and binder during processing (printing or molding, depending on the process used). This encourages isotropic shrinkage during debinding and sintering, which improves the quality of the final parts [20, 39, 65, 71]. Separation of the feedstock components during processing can result in part distortion, uneven or excessive porosity, and cracks in the final sintered parts [72]. Various techniques during feedstock preparation can help with this problem; some examples include twin screw mixers [51], Z-blade mixers [47, 51, 65, 73], and twin-roll mixing mills [52]. For materials that tend to agglomerate, a co-rotating screw mixer, followed by mechanical screening, can be very effective due to high shear [53, 54].

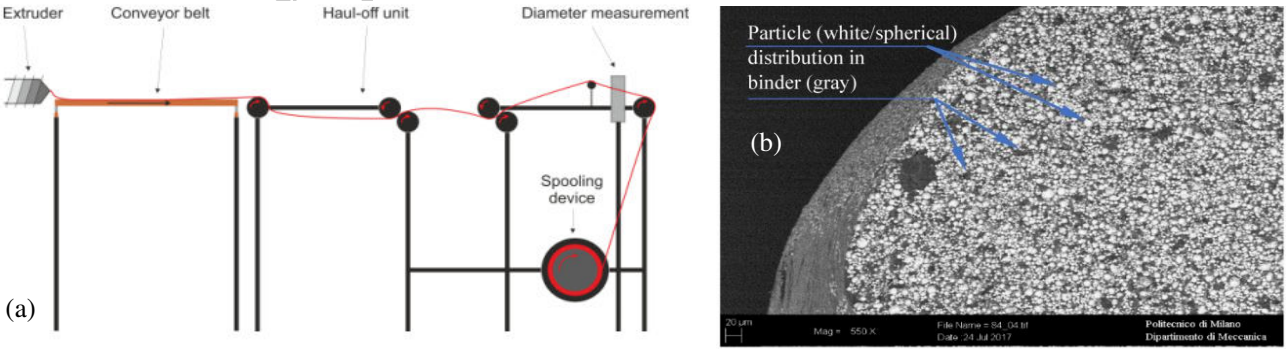

Figure 4: (a) PME filament production process diagram [29] and (b) example green printed part with excellent powder distribution [74]. Panel (a) reproduced under terms of a CC-BY license and panel (b) © Elsevier B.V., reproduced with permission.

.

Some specific considerations are required when manufacturing filament for PME beyond what would be required for molded parts or pellets. The main concerns are the heaviness, the relatively small filament diameter,

and the increased brittleness due to the high powder content. The process starts off similarly to the regular process for manufacturing MEAM filament, with the ingredients (powder plus binder components) being mixed by a screw and driven to the die through several heating zones [6, 29, 40]; this mixing and processing is the norm whether or not the ingredients are pre-mixed or not. Due to the properties of the binder and powder mix, it is important to monitor the pressure via a rheometer [21, 61]. Normal MEAM filament can often be spooled directly from the extruder die, but PME filament requires the use of a conveyor belt (similar to metal extrusion) [6, 29, 32] before being carefully spooled in a way that does not damage the brittle filament (Figure 2a and Figure 4a). In general, a pre-warmer [7, 17, 41, 43] is required to unspool the filament without breaking it. Due to its properties and printing behavior, the filament must be subject to strict dimensional standards, both in terms of diameter and ovality [27, 61, 62], where the ovality is defined as the difference between the diameter in the horizontal direction and the diameter measured in the vertical direction. The correct diameter is an essential parameter for selecting correct and effective flow rates during PME printing; inconsistency in diameter can cause gaps in the print (which will be magnified during sintering) or over-flow which can waste material and cause clogs and failed prints [22, 40, 47]. To avoid filament buckling and compression during printing, the force transmitted from the wheels of the extruder drive to the filament must be adequately transmitted to the center of the extrusion nozzle in the direction of melt flow, with the minimum loss. Rane et al. [74] noticed that with increased powder content, the distribution of powder throughout the filament is more uniform and the surface of filament transformed to be smooth, resulting in improved isotropy. Figure 4b shows an example of a printed element with an excellent powder distribution.

4. Debinding Methods

4.1. Debinding Objectives

The primary objective of the debinding process is to remove the primary binding polymer components from a part which is built using a powder or particles held together with a polymer binder. This removes as much of the binder as possible, so effective particle welding can occur during sintering without interference from impurities, particularly carbon residue [7, 48, 70, 75]. Since the backbone remains after debinding, the parts do not disintegrate back into raw powder during the process. Debinding is used in combination with a wide variety of different manufacturing processes, such as PIM, PM, and PME to prepare these parts for sintering and final use. A green part that has been manufactured and then debinded, but not yet sintered, is known as a *brown* part [7, 76]. The process used for debinding is specific to each combination of materials in the green part, but will generally fall into one of four categories: Thermal debinding (using heat to remove the primary binder) [70], solvent debinding (using a solvent (usually organic solvents like heptane or hexane) to remove the primary binder) [77], water debinding (removing the binder by dissolving and washing with water - a special case of solvent debinding) [78], and catalytic debinding (removing the binder using a catalytic acid vapor) [79]. The choice of debinding method may be made after manufacturing of the parts or could be a consideration during the feedstock manufacturing, where a specific debinding method can drive the composition of the binder. As discussed later in this paper, all four debinding methods could be effectively applied to PME-manufactured parts. The review found that three of them have already been applied widely and successfully.

4.2. Thermal Debinding

The most common and straight-forward method to remove the binder from parts is to melt or thermally degrade it, especially when the binder is a thermoplastic polymer. During this process (Figure 5a), the part is heated slowly and in a pattern (for example, as shown in Figure 5b) appropriate for the material and binder being used [70, 73, 80, 81]. A programmable furnace, such as the example shown in Figure 5c, is generally used so that the needed thermal cycle can be accomplished with minimal supervision and interruption. To prevent oxidation and other problems during debinding, the part must be isolated from the air; this may be done using a shielding gas or burying the part in a refractory such as aluminum oxide (Al_2O_3), activated charcoal, or talc powder [17, 70, 80–85], which is sometimes known as "wicking". Care must be taken to avoid trapped gasses or areas of binder that were not completely degraded during the debinding, as these can cause severe defects in the part during sintering. This is especially an issue when debinding thick parts, so great care must be taken to ensure full penetration of the heat into the part to remove the binder [7, 86, 87].

During the thermal process, the polymer binder is softened and then removed, so the (now brown) part becomes more brittle and more subject to cracking and other defects [70, 82, 86, 87]. Thermal debinding is at least partially dependent on thermal degradation, even in cases where part of the main binder can be melted

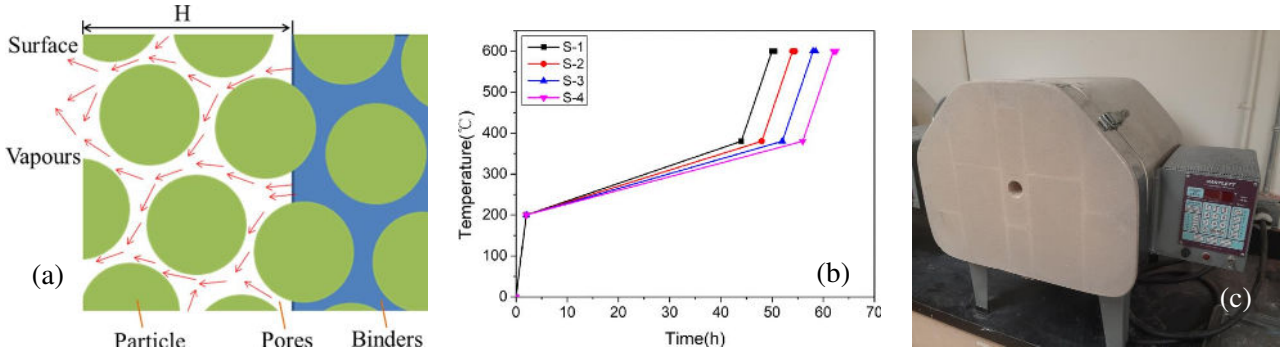

Figure 5: (a) Process diagram for thermal debinding, showing the various system components affected [80]. Panel (b) shows a typical debinding thermal cycle [80]. An example of a typical debinding furnace is shown in Panel (c). Panels (a)-(b) © John Wiley and Sons, Inc., reproduced with permission. Panel (c) original to this article.

.

Table 4: Examples from the reviewed literature that used thermal debinding on parts made using PME. PTB = Proprietary thermoplastic binder (unspecified composition). SS indicates stainless steel alloys. See Table 3 for binder types.

Case	Powders(s)	Binder	Powder %	Debinding Process
Abe et al. [9]	17-4PH SS	POM, PP, PW	60	Thermal debinding at 600°C in a nitrogen gas atmosphere for 2 hours.
Agarwala et al. [47, 88, 89]	Si_3N_4	PTB	55	Thermal debinding completed in two stages, the first in an a nitrogen atmosphere at 450°C and the second at 200°C in a bed of activated charcoal.
Cerejo et al. [8]	316L SS	POM, TPE, LDPE	60	Thermal debinding at 600°C (heat rate 1°C/s) in a hydrogen atmosphere.
Conzelmann et al. [90]	Al_2O_2	EVA, SA	50	Thermal debinding in two steps, the first one at 230°C for 8 hours and the second at 1000°C for 2 hours. The samples were buried in a $PbZrO_3/ZrO_2$ powder bed.
Kurose et al. [91]	316L SS	POM, PW	60	Thermal debinding at 600°C in a nitrogen atmosphere for 2 hours.
Mousapour et al. [92]	316L SS and high-carbon steel	PLA	83	Thermal debinding in an argon atmosphere at a heating rate of 1°C/min to 400° with a 1 hour hold. Samples hung from a wire in the furnace.
Renukaradhya [93]	316L SS	PTB	83	Thermal debinding at 450°C in a hydrogen atmosphere.
Riecker et al. [94]	316L SS	PA, PLA	50	Thermal debinding at various temperatures.
Sadaf et al. [95]	316L SS	LDPE	65	Thermal debinding at 500°C in a hydrogen atmosphere
Santos et al. [96]	Copper	PO, TPE	61	Thermal debinding at 500°C in an argon-hydrogen atmosphere.
Terry [97]	Copper	PLA	90	Thermal debinding at 500°C for 4 hours in an open furnace with sintering ballast to prevent oxidation.
Wang et al. [98]	316L SS	PE, SA	80	Thermal debinding at 200°C for 2 hours and 425°C for 1 hour.

away. During thermal degradation, the most important considerations are the heating rate, the temperatures at each milestone (e.g., Figure 5b), and the amount of time each temperature is maintained [70, 73, 80, 81, 85]. One of the most widely used method for tracking the progress of thermal degradation is the thermogravimetrical

analysis (TGA) technique. The TGA method is described in Appendix A for interested readers. In decomposition reactions, the mass of the reactants decreases and is often substituted by an increase in the mass of solid output products. Therefore, TGA is based on the real-time total mass of the system as it changes during thermal cycling (controlled heating or cooling). This mass can be obtained either as a function of temperature change or as a function of time in a controlled environment [20, 39, 99–101]. Examples of successful thermal debinding of parts made with PME from the reviewed literature are shown in Table 4. The reviewed papers show that a range of ceramic and metal parts, with many different binders (Table 3) can be successfully prepared for sintering using thermal debinding with only standard equipment.

4.3. Organic Solvent Debinding

In contrast to the relatively simple and straight-forward thermal debinding process, solvent debinding (Figure 6a) can be quite complex and require great attention to detail. While thermal debinding can be used to prepare the part for sintering directly, solvent debinding usually requires the part to be debinded in two steps, the first one to dissolve most of the binder and the second to thermally degrade the remaining polymers. This heating step usually takes much less time than direct thermal debinding. Solvent debinding is more or less effective than thermal debinding depending on the composition of the binder; some more complex binder compositions may require the use of solvent debinding, as thermal debinding would not be able to properly prepare the part for sintering. The solvent extraction rate is a dissolution and diffusion process. Therefore, it is dependent on the temperature, time, and characteristics of the particles such as the shape, size, and distribution of the powder. Feedstocks designed for solvent debinding have at least two kinds of binders. The initial binder, called the *solvent binder*, is eliminated from the inside of the part by the solvent, creating a network of pores and inclusions that connect to each other [31, 102, 103]. Some of the solvents used in the literature have been ethanol [104], cyclohexane [105], heptane [106], water at different immersion times and temperatures [60, 104, 106–108] (see next section on water debinding). The binder ingredient extracted by the solvent must be attached to the compact surface. For adequate interconnectivity, the binder should have at least 30% soluble ingredients. The amount of debinding relies upon molecular mobility, which is faster with elevated temperatures and smaller solvent molecules [106, 109].

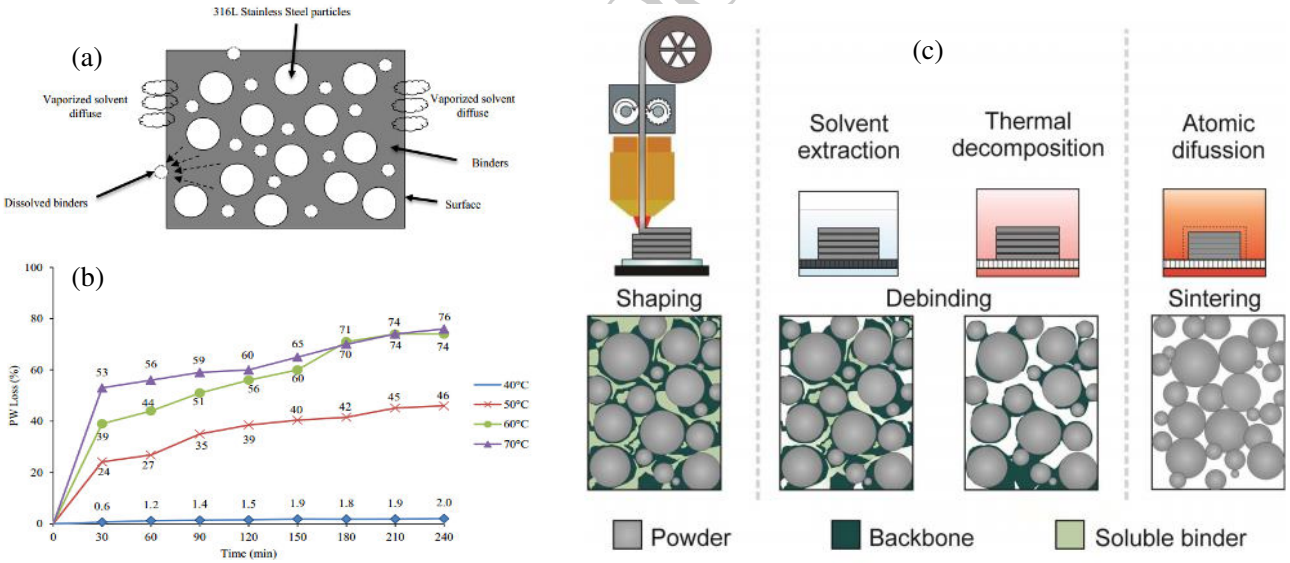

Figure 6: (a) Schematic of the solvent debinding process [106], (b) an example of binder removal rate as a function of solvent temperature [106], and (c) example process steps for solvent debinding of PME parts in combination with a thermal process [22]. All panels reproduced under the terms of a CC-BY license.

.

Solvent debinding is generally faster than thermal debinding [106, 110], but is much slower than catalytic debinding; however, the cost and environmental risk are much lower than seen with catalytic debinding [75, 108]. During solvent debinding, the temperature and immersion time of the parts inside the solvent are critical and must be optimized to obtain the maximum density during sintering. In general, a higher immersion temperature leads to a faster degradation of the binder [106, 111] (Figure 6b). However, care must be taken as it has been

observed that immersion temperatures above 61°C decreases the green part density and leads to the swelling for some materials; the high immersion temperature encourages the formation of larger pores between the powders and the binder system in order to the decomposition of the polymer in the green part. Polymers pass through empty space and soluble molecules enter into the debinded part [112]. The solvent liquid needs to be renewed continuously to prevent part saturation [7]. Figure 6c shows the process steps for solvent debinding applied to PME [22].

After the soluble binder component is removed from the part, sometimes it must be heated to remove the backbone polymer while maintaining the geometry for sintering [36]. This thermal phase can be done in the sintering furnace and is usually done at a temperature between 200°C and 600°C for 2-4 hours, which are high enough to degrade the polymer without damaging the powdered metal or ceramic component [39, 103, 106, 110, 113]. It is vital that both binder components be removed as much as possible, as remaining binder can cause swelling, cracking, and other problems during sintering [106, 112]. Parts with a low volume-to-surface area ratio tend to work best for solvent debinding, due to the easier removal of the maximum amount of binder relative to the time and energy required for debinding [110]. Mass loss of the binder (M_{loss}) is determined [106, 114] as:

$$M_{loss} = \frac{(M_i - M_f)}{M_i} \times 100 \tag{1}$$

where M_i is the mass of green part and M_f is the mass of brown part after debinding. By increasing the degradation temperature, the percentage of the main body loss of the green compacts can be increased [106]. The solvent debinding rate can be described as:

$$t = \frac{H^2}{\beta} \ln\left(\frac{V_B}{1-\phi}\right) e^{(Q/KT)} \tag{2}$$

where t is the debinding time, H is the section thickness, T is the temperature, V_B is the fraction of binder to be removed, β is the binder solubility factor, ϕ is the factional solid loading, Q is the activation energy for binder solution into the solvent, and K is the Boltzmann Constant.

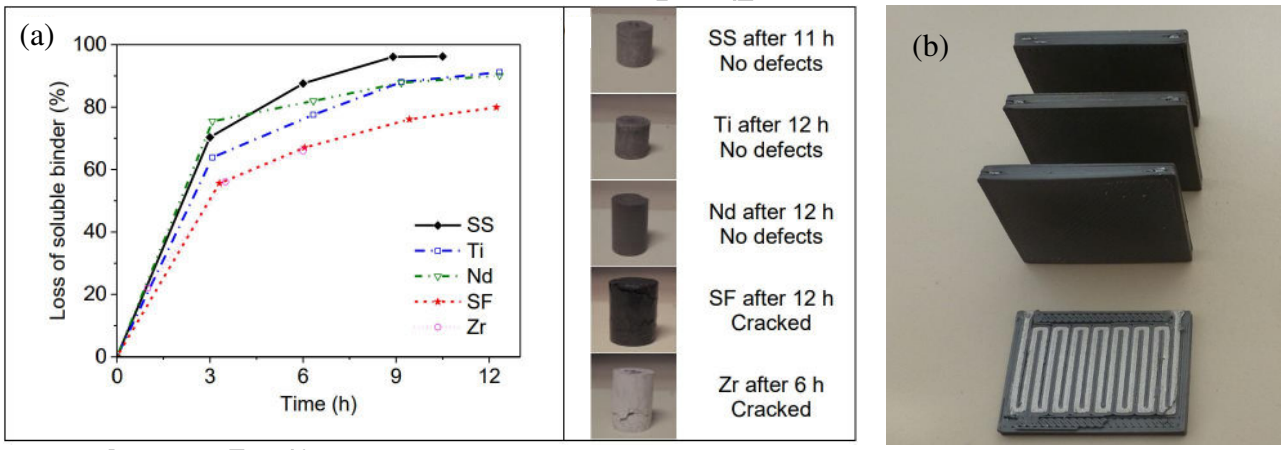

Figure 7: (a) Example binder loss curves for different material feedstocks, with examples of debinded material samples [60] and (b) examples of hybrid metal-ceramic composite materials manufactured using PME and solvent debinded [6]. All panels reproduced under the terms of a CC-BY license.

A good example of the complete solvent debinding process applied for a single specific material with different binder systems was presented by Cano et al. [27]. In this work, PME was done using zirconia powder. The main binder system composed of a acrylic acid-grafted high-density polyethylene SCONA TPPE 2400 (AA-HDPE, BYK-Chemie GmbH, Germany). The zirconia powder had a large surface area and a tendency to agglomerate, so stearic acid was used as a second component (SA, Merck Schuchardt OHG, Germany) to promote particle dispersion in the binder and prevent re-agglomeration. An amorphous polyolefin (APO) and a styrene ethylene/butylene-ethylene copolymer (SEBS) were tested as single soluble components. The incorporation of paraffin wax (PW) or extender oil (EO) as a second soluble component was also assessed. The binder system containing SEBS and PW had the best ultimate tensile strength and secant modulus, a low viscosity. The incorporation of zirconia powder boosted the viscosity, strength, and stiffness of the combination, while sharply

reducing the flexibility (i.e., increasing the brittleness). While the formulations exclusively including SEBS had the most favorable mechanical properties, the incorporation of PW as a low-viscosity and soluble ingredient was essential to diminish the viscosity and the number of defects that are apparent after solvent debinding. The filament made of SEBS/PW could be processed by PME and the printed parts had no visible defects after debinding and pre-sintering. In the debinding step, specimens were immersed in pre-heated cyclohexane at 60°C for 6 hours, with 12 ml of solvent per gram of binder. After 6 hours in the solvent, the specimens were dried in the vacuum drying oven Binder VD 23 (Binder GmbH, Germany) at 80°C for at least 2 hours.

Table 5: Powders used for Kukla et al. [60] study in solvent debinding.

Powdered Material	Particle Shape	Particle Size (μm)	Powder Content (%)	Abbreviation
316L Stainless Steel	Spherical	6.05	55	SS
Ti6Al4V	Spherical	14.97	55	Ti
NdFeB	Irregular	28.29	55	Nd
SrFe12O19	Irregular	1.35	55	SF
Zirconia	Irregular	0.6	50	Zr

Direct comparison of the performance of several base (powdered) materials against each other during solvent debinding was done by Kukla et al. [60]. In this study, five different materials (316L stainless steel (SS), Ti6Al4V (Ti), NdFeB (Nd), SrFe12O19 (SF), and zirconia (Zr)) were explored (Figure 7a). Table 5 shows some specifications for these powders. The binder composition was kept constant and composed of a thermoplastic elastomer, polyolefin, and dispersible/compatible materials. Two types of equipment were used to produce the feedstock; for small amounts, an internal mixer (Brabender Plasticorder PL2000) was utilized, while for larger quantities a twin-screw extruder (Leistriz ZSE 18 HP-48D) was employed. After compounding, the feedstocks were granulated in a grinder with a squared sieve with 2 mm orifices. Cyclohexane was used for the solvent at 60°C to remove the polymer binder. To control the temperature, a rotating oil bath with heater controllers was utilized. The solvent extraction of the main binder ingredient was clearly influenced by the used powder. Figure 7a shows the amount of soluble binder loss as a function of time. The stainless steel had the most rapid debinding through all materials examined. Nd is debinded faster than Ti, but mass loss of two materials is very similar over time. The two fast ceramic powders considerably decreased the rate of binder separation, likely driven by powder size (Table 5). Smaller irregular particles have a larger surface area that the polymer can adhere to and create smaller pores between the particles, decelerating the release of solvent into the compacts. The debinded samples shown in Figure 7a suggest that the filler material used in the feedstock can cause damage during debinding with the settings and binder used in this study. Ceramic-filled feedstocks result in the crack; however metal-filled feedstocks can be debinded without damage. Thus ceramic feedstocks require careful adjustments in binder formulation and processing conditions.

Table 6: Examples from the reviewed literature that used solvent debinding on parts made using PME. The three detailed cases discussed in this section are not included in this table. PTB = Proprietary thermoplastic binder (unspecified composition). SS indicates stainless steel alloys. See Table 3 for binder types.

Case	Powders(s)	Binder	Powder %	Debinding Process
Burkhart et al. [36]	316L SS	PTB	55	Solvent debinding using cyclohexane at 60°C.
Fan et al. [115]	Al_2O_3	EVA, PP, PW, SA	40-75	Solvent debinding was done in heptane for 3 hours at 80°C followed by thermal degradation at an unspecified temperature and environment.
Gonzalez-Gutierrez et al. [29]	316L and 17-4PH SS	PTB	55	Solvent debinding using cyclohexane at various temperatures, followed by thermal degradation at 550°C in an argon-hydrogen atmosphere.

Continued on next page

Table 6 – continued from previous page

Case	Powders(s)	Binder	Powder %	Debinding Process
Gonzalez-Gutierrez et al. [34]	17-4PH SS	PTB	55	Solvent debinding using cyclohexane with varied temperatures, followed by thermal degradation at 650°C in a nitrogen/hydrogen atmosphere.
Gonzalez-Gutierrez et al. [35]	316L SS, 17-4PH SS, Ti6Al4V, YSZ, NdFeB	PTB	55-60	Solvent debinding using cyclohexane at 60°C.
Gonzalez-Gutierrez et al. [30]	17-4PH SS	PO, TPE	55	Solvent debinding using cyclohexane at 70°C, followed by thermal degradation 600°C in hydrogen atmosphere.
Gonzalez-Gutierrez et al. [45]	Copper	TPE, PP	55	Solvent debinding using cyclohexane at 60°C for 24 hours, followed by thermal degradation in a hydrogen atmosphere at 450°C for 2 hours.
Kan et al. [37]	316L SS	PP, PW, SA, SEBS	50	Solvent debinding using cyclohexane at with varied temperature and debinding time, followed by thermal degradation at varied temperature and processing time. Hydrogen and hydrogen-argon atmosphere used for thermal processing.
Naranjo et al. [13]	M2 high speed steel	PO, TPE	60	Solvent debinding using cycloalkane at 65°C, followed by thermal degradation in a nitrogen atmosphere at 450°C for 1 hour.
Notzel et al. [48]	Al_2O_3	PW, LDPE	10-60	Solvent debinding in n-hexane, followed by thermal degradation at 500°.
Singh et al. [20]	Ti6Al4V	PTB	59	Solvent debinding using n-heptane at 64°C for 4 hours, followed by thermal degradation in a vacuum chamber at various temperatures and processing times.
Suwanpreecha et al. [116, 117]	17-4PH SS	PTB	63	Solvent debinding using a mix of unspecified commercial debinding fluid and trans-1,2-dichloroethylene in a bath for 12 hours, followed by thermal degradation at 450°C for 100 minutes in an argon-hydrogen atmosphere.
Thompson et al. [7]	316L SS	PO, TPE	55	Solvent debinding using cyclohexane at 65°C for various debinding times, followed by thermal degradation in a vacuum chamber at 750°C for 1.5 hours.
Thompson et al. [11]	Pure titanium	PO, TPE	55	Solvent debinding using cyclohexane, followed by thermal degradation in a vacuum chamber or argon atmosphere at various temperatures.
Wagner et al. [38]	316L SS	LDPE, TPE, SA	50	Solvent debinding using cyclohexane at 60°C, followed by thermal degradation at varied temperature in a hydrogen atmosphere.
Zhang et al. [39]	Ti6Al4V	PO	55	Solvent debinding using acetone at 60°C for 24 hours, followed by thermal degradation at different temperatures and heating rates.

Solvent debinding of parts containing both metal and ceramic powder (requiring careful balancing of the parameters, as demonstrated by Kukla et al. [60]) was explored by Abel et al. [6]. The parts (shown in Figure 7b, were manufactured using PME out of 17-4 stainless steel and zirconia. The binder used was a mixture of thermoplastic polyolefin and stearic acid, but since the filament used was proprietary, not much information

was given in the study. The solvent material was cyclohexane at a temperature of 60°C, with a treatment time of 8 hours. Due to the conditions of the materials and the amount of binder left, it was necessary to use a thermal degradation process (in an argon atmosphere to prevent oxidation) after the solvent debinding in order to fully prepare the parts for sintering. Using a maximum temperature of 440°C and different heating rates between 5°C/h and 150°C/h, and all different samples showed no significant deformation or bloating. While the study report was lacking some technical details, the results show that it was successful in combining metal and ceramic parts using PME.

These three cases demonstrate the complex decision-making process and preparation required to use organic solvent debinding. However, in spite of the difficulty in using it, this approach was the one most commonly used in the literature. Table 6 shows a large variety of other cases where organic solvent debinding (with or without a thermal degradation step) was used successfully for PME parts. Both metals and ceramics are well-represented in these studies. It was noted that the cases where organic solvent debinding was successful, the ratio of powder to binder was lower than those observed for thermal or catalytic debinding. This is consistent with the previous knowledge from PIM and other powder processes that the solvent works best when the spaces between the powder particles is larger and therefore more accessible to the solvent.

4.4. Water Debinding

Water debinding is a special case of solvent debinding, where an aqueous solution is used to remove the binder instead of an organic one [104, 118]. While its use is restricted to water-solutable binders, it is preferable to organic solvent debinding where applicable, as it is clearly safer and more environmentally sustainable, as well as being more effective for some binder polymers. Common water-soluble binders include polyethylene glycols, polyethylene oxides, polyvinyl alcohols, starches, and polyacrylamide [78, 119–122]. The capability of water to penetrate the outer surface of the components depends on the bonding elements and the chemical interaction of those parts [66]. Water is effective in removing these polymers, due to the fact that these polymers contain monomers that include oxygen and nitrogen, which are hydrophobic [119, 123]. Similarly to standard solvent debinding, the water debinding time is related to powder material, water temperature, water circulation, particle size, component geometry, and water volume relative to the "green part" mass. All of these variable parameters interact with each other and require to be optimized for each specific component. After water debinding, the parts must placed in a vacuum or forced air furnace (Figure 8a) for several hours to ensure complete drying and to complete thermal degradation before the weight loss (calculated as shown in the previous section) can be measured [7, 11, 119, 123–125]. It is clear that temperature plays a fundamental function in the flow and mobility of polymers; this is an important consideration for water debinding, as the the rate of binder removal is enhanced by boosting the temperature of water bath [124]. However, very rapid removal of the binder has been noted to cause a reduction in mechanical strength of the brown part and can cause warping and other distortions. Therefore, it is generally not a good idea to use very high water bath temperatures during water debinding [126]. Due to the larger space between the particles, green parts made with larger or courser powder are faster and easier to debind using aqueous solvents than corresponding parts with finer powder [127, 128].

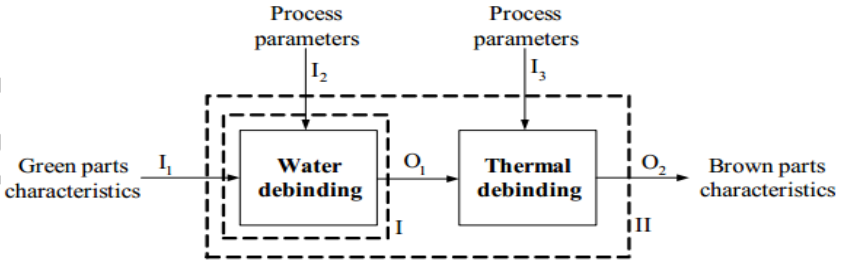

Figure 8: (a) Example process where water debinding is used in combination with thermal debinding [111]. Reproduced under the terms of a CC-BY license.

During this review, no examples of water debinding were found using parts made using PME. However, this debinding method is commonly used for PIM parts [111, 119, 129] and therefore is potentially useful for PME parts using water-soluble binders.

4.5. Catalytic Debinding

The final major debinding method covered in this review is catalytic debinding, during which the main binder is removed by being attacked directly by a catalytic acid vapor [79, 130, 131]. The binder mass is removed primarily by being converted into a vapor by the catalyst and then blown away [65, 129]. The polyacetal molecule is key for the success of this process [32, 33, 64, 79, 132, 133]; the molecular structure of polyacetal consists of the continuous repetition of the oxygen-carbon chain, as shown in Figure 9a. The oxygen atoms in the polymer chain are prone to acid attack and cause the polyoxymethylene macromolecules to convert into formaldehyde when exposed to a suitable acid catalyst [18, 22, 102]. Figures 9b-c show examples of polyacetal networks before and after debinding. Formaldehyde has a low molecular weight and is quickly removed from the interface of binder and vapor [64, 79, 132, 134]. The catalyst most often used for the degradation process is nitric acid gas with a purity of more than 98.5% [32, 33, 108]. As a result, the polymer binder system in the catalytic method is eliminated faster than the thermal and solvent methods. The catalytic debinding approach (Figure 10a) generally produces a well-interconnected porosity after a short time (about two or three hours depending on the size of the component - Figure 10b) [108].

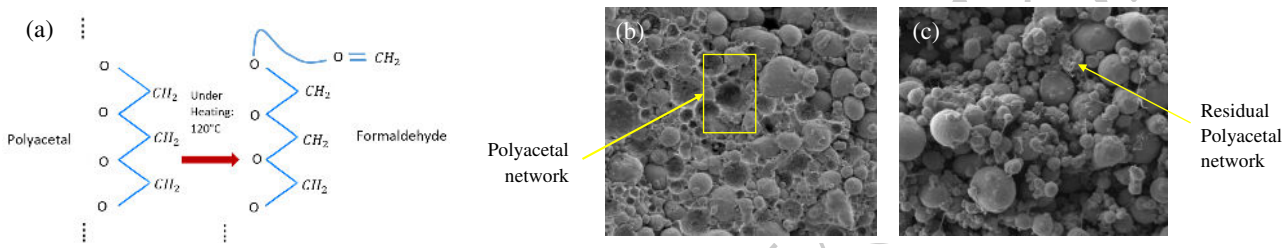

Figure 9: (a) polyacetal chemical analysis, (b-c) SEM image of stainless steel 316L before (b) and after (c) catalytic debinding. All panels original to this article.

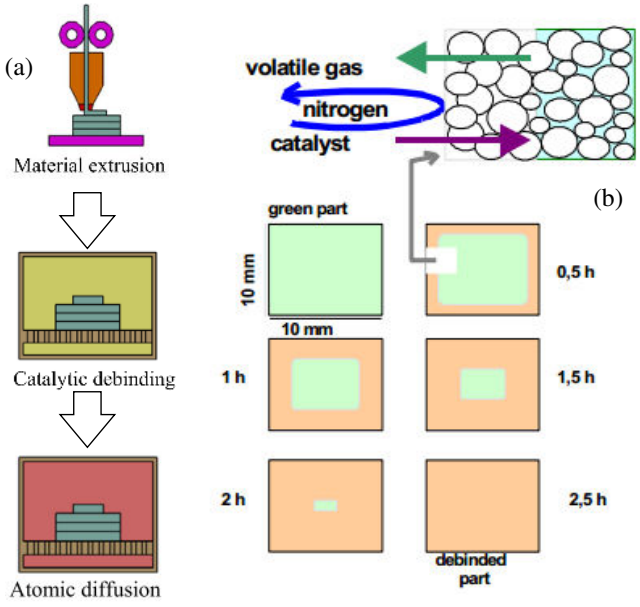

Figure 10: (a) placement of catalytic debinding within the PME process [1], (b) example catalytic debinding progress as a function of time [132]. Panels (a) and (b) reproduced under the terms of a CC-BY license.

It should be noted that in both solvent (including water) and catalyst debinding methods, a fraction of insoluble polymer that is resistant to solvent or acid remains in order to have sufficient strength and retention of the part until the start of sintering (usually about 10% of the total weight of the binder). This residual polymer, depending on its chemical composition, is usually removed between 200°C and 600°C in the pre-sintering stage [31, 33, 65, 142]. Increasing the cooling rate causes thermal stresses and cracks in the printed

Table 7: Examples from the reviewed literature that used catalytic debinding on parts made using PME. PTB = Proprietary thermoplastic binder (unspecified composition). SS indicates stainless steel alloys. See Table 3 for binder types.

Case	Powders(s)	Binder	Powder %	Debinding Process
Ait-Mansour et al. [135]	316L SS	POM, PP, DOP, DBP	80	Catalytic debinding in nitric acid at 110°C, followed by thermal degradation at 600°C for 1 hour at a heating rate of 5°C/minute.
Caminero et al. [136]	316L SS	PTB	80	Catalytic debinding in nitric acid at 120°C for 8 hours, followed by thermal degradation at 600°C for 1 hour at a heating rate of 5°C/minute.
Damon et al. [33]	316L SS	POM, PP, DOP, DBP	88	Catalytic debinding, followed by thermal degradation in hydrogen atmosphere at 600°C for 1 hour at a heating rate of 5°C/minute.
Gong et al. [31]	316L SS	POM, PP, DOP, DBP	88	Catalytic debinding completed by professional debinding and sintering company. Debinding details not provided.
Jiang & Ning [137, 138]	316L SS	POM, PP, DOP, DBP	88	Catalytic debinding in nitric acid at 120°C, followed by thermal degradation at with varied temperatures for 1 hour at a heating rate of 5°C/minute.
Liu et al. [139]	316L SS	POM, PP, DOP, DBP	88	Catalytic debinding in nitric acid at 120°C, followed by thermal degradation at 600°C for 2 hours at a heating rate of 5°C/minute.
Quarto et al. [140]	316L SS	POM, PP, DOP, DBP	90	Catalytic debinding in nitric acid at 120°C.
Rosnitschek et al. [141]	316L SS	POM, PP, DOP, DBP	88	Catalytic debinding in nitric acid with varied processing temperature, followed by thermal degradation at 600° for 1 hour at a heating rate of 5°C/minute.

part. If the thickness of the parts is above 4 mm, after the completion of debinding, the oven must be cooled to 70°C before opening it [18, 132]. The normal debinding velocity at 110°C is between 1 mm per hour and 2 mm per hour, as can be seen in Figure 10b [18, 132]. If the number of loaded parts inside the oven is higher, the debinding time increases. Placing parts in the oven more than the minimum debinding time generally has no effect on the parts; binder degradation temperature, purity percentage, catalyst feed rate, and carrier gas feed rate are the parameters affecting the debinding velocity [134]. The distance between the parts should be large enough for the gases to be exchanged. By placing the parts on a perforated sheet, the debinding time can be shortened because acid nitric gases can easily reach the bottom surface of the parts.

The debinding rate can be increased with increasing nitric acid flow rate [132, 134] but high nitric acid injection increases the concentration of oxidizing gases and formaldehyde from degradation, which in many cases can lead to combustion. The main function of nitrogen gas in this process is as a carrier in the chamber of the oven before starting the process of degradation in order to exhaust the oxygen, because if there is oxygen and formaldehyde, the reaction of these two substances together causes an explosion [102]. Nitrogen gas is also the carrier gas for extracting gases from the decomposition and sublimation of polyacetal [134, 143]. For a better catalytic reaction, the ratio of nitric acid to nitrogen gas must be below 4% [102]. Although liquid nitric acid is highly oxidized, anhydrous acid vapor does not react with most metal powders used, such as iron, nickel, chromium, molybdenum, silicon, titanium, Al_2O_3, ZrO_2, and Si_3N_4. Cobalt, copper, and copper alloys are oxidized in an acidic debinding atmosphere. The acidic catalyst is injected into the oven utilizing a ceramic piston pump. The ovens used in catalytic debinding have corrosion-resistant internal surfaces against nitric acid [134]. This system cannot be used for hard metals due to oxidation or conversion to nitrate powder such as cobalt powder oxidation by nitric acid gas. Oxalic acid [144], as a strong volatile organic acid, causes rapid decomposition of polyacetal, which does not contain any elements such as halogens, sulphur, or phosphorous, which may contaminate the sintered parts. It is generally more suitable than 100% nitric acid [134, 143].

Similar to the thermal and organic solvent debinding, catalytic debinding has been used for several studies related to PME. These are shown in Table 7. Unlike the other two, which worked with a diverse range of different powders and binders, catalytic debinding has really only been applied to stainless steel parts and some specific binders. As shown in the table, the debinding process for all the cases were very similar. This suggests that

Table 8: Trade-off table for debinding methods. It is assumed that all of the methods can successfully debind both metal and ceramic green parts.

Process	Advantages	Disadvantages
Thermal Debinding	• Simple operation with common equipment • No hazardous chemicals needed • Low environmental impact beyond energy consumption • Wide variety of environments possible • Can be used in combination with other debinding processes as needed • Minimal training required for use • Only basic PPE required for users • Works well for parts with high powder content	• Slow process • Must have a clean and oxygen-free environment • Less effective than solvent debinding for some binders • May introduce stresses into the debinded parts due to thermal cycling • Due to thermal stress on the parts, parts made by combining ceramic and metal powder are not possible
Organic Solvent Debinding	• Relatively fast process • Cleanliness and preparation of the parts is not as important as in thermal debinding • Very flexible process, can process a wide variety of powders and binders • Can process green parts that are made from both metal and ceramic powder • No thermal cycling or stress introduction (in chemical phase)	• Very complex process that requires careful planning • There is a risk of chemical reactions between the parts/binders and the solvent • Extensive user training and PPE needed • Some of the chemicals used are very hazardous to the user and environmentally hazardous • Does not work well for high-powder green parts • Usually requires a thermal degradation step before sintering due to residual binder • Parts must be thoroughly and fully dried before sintering
Water Debinding	• Similar to organic solvent debinding, except does not require hazardous chemicals or PPE for the user	• Similar to the organic solvent debinding process, except the application range is much smaller and is limited to parts with water-soluble binders • In the reviewed literature, water debinding has not been used successfully for PME parts
Catalytic Debinding	• By far the fastest debinding process used for PME • Simpler to use than solvent debinding • Can be used with parts made with a high powder density	• The processing environment is sensitive to its setup • The gasses used are potentially hazardous and environmentally dangerous • Extensive training and PPE required • Limited to only some materials and binders due to the oxidation and other chemical reaction risk of the material with the acid gas

the catalytic debinding process has a limited application range, but it was found to be very fast and effective for the cases where it was used. It also seemed to be very effective for parts with a very high powder content, unlike the solvent debinding methods; this is likely because the gas has an easier time penetrating into the pores of the part to reach the binder than what would be seen with a fluid. The fast reaction of the catalyst tends to remove the binder so fast that the parts can collapse if this is not controlled for; therefore, applications with high powder density seems to be the best application of catalytic debinding.

4.6. Comparisons Between Different Debinding Processes

One of the major research questions for this review was how the different debinding methods compare with each other, both for general use and specifically for PME. Table 8 shows the results in the form of a table directly comparing the advantages and disadvantages of each process. This information was used to create a decision stoplight chart (Table 9) for the processes, comparing performance in several major areas (processing speed, process complexity, environmental impact, process flexibility, user safety, and the ability of the process to work with a variety of different metal, ceramic, and mixed powders. The powder density of the green PME parts that each process was shown to successfully work with is shown in Table 10. This information was collected from and summarized here from the previously cited works.

Table 9: Decision stoplight chart for debinding methods. Attributes are processing speed [Speed], process complexity [Complexity], environmental impact [En. Impact], process flexibility in terms of the binders and materials used [Flexibility], process safety [User Safety], and the ability of the process to work with metal, ceramic, and mixed parts [CerMet]. Red indicated poor or negative, green indicates good or positive, and yellow indicates a moderate or restricted attribute.

Process	Speed	Complexity	En. Impact	Flexibility	User Safety	CerMet
Thermal Debinding	Slow	Low	Low	Medium	Some hazards	M, C
Organic Solvent Debinding	Medium	High	Medium	High	Some hazards	M, C, mix
Water Debinding	Medium	Medium	Low	Low	High	M, C, mix
Catalytic Debinding	Fast	Medium	High	Low	Some hazards	Limited M, C

Table 10: Powder density range for each debinding method from the reviewed literature. Water debinding was not included, as no examples of water debinding for PME parts were found during the review.

Process	Less than 40%	40-50%	50-60%	60-70%	70-80%	80-90%	90%+
Thermal Debinding							
Organic Solvent Debinding							
Catalytic Debinding							

5. Defects and Quality Issues in Debinding

According to the reviewed papers from this study (previously referenced), defects in debinded parts can come from five major sources:

1. Trapped binder that is not removed during the debinding process
2. Poor mixing quality and uniformity in the feedstock
3. Selecting the wrong debinding process for the given base material and binder, resulting in ineffective debinding or chemical reactions between the binder/powder and the gas or fluid used to debinding
4. Using the wrong process settings or stopping the debinding before the process is complete
5. Thermal shock, especially for parts that have delicate, thin, or overhanging features

In well-made PME feedstock, the binder and powder are mixed uniformly with no air gaps in the structure. Ideally, during the debinding process, the polymer components are removed and leave only the metal or ceramic powder in approximately the same position as before debinding. This allows the powder to properly consolidate during sintering. In thermal and catalytic debinding, gasses from the removed polymer need to be able to properly escape, while in organic solvent and water debinding require that the fluid be able to get out of the part structure. Poor connectivity of the pores in the structure can result in parts of the binder remaining

in the parts after the debinding procedure is complete, resulting in the gas or fluid that is trapped inside causing bloating or cracking of the parts. Where the feedstock is of poor quality or has been softened due to age, humidity, or exposure to water, similar defects can appear, both during the debinding process and during sintering. When the powder is not mixed uniformly in the feedstock, part orientation and the effect of gravity can have an effect on the quality of the polymer removal. In addition, the uneven heating and mass of the material can introduce residual stresses into the part before sintering. This is especially an issue with lower-powder parts (40-80%), as the significant shrinkage of the part during sintering will service to expose and amplify the defects. In solvent debinding, cracking, and slumping commonly happen when the process settings or time are not appropriate. Warpage and slumping frequently occur, particularly when the part has a complicated shape with overhanging sections. To solve this problem, using a stronger backbone binder and a lower debinding temperature is usually beneficial. A modification of the part shape to give better support for thin or extended sections is also commonly employed. Poor bonding between binder and powder, low strength of backbone binder, and large differences in section thicknesses can lead to the creation of cracks as well. In order to solve these problems, one can change the type and composition of solvent or binder, parts designs with smaller differences in section thicknesses, and using lower debinding temperature. In thermal debinding defects are frequently seen when the applied heating rate is too fast. The 100% thermal debinding is a slow process since decomposed gas components that develop in the core section cannot escape to the atmosphere effectively through any pore channels. Defects are frequently encountered unless extremely slow heating rates are used with long debinding times. Figure 11 shows some examples of errors and technical problems that can arise during or immediately after debinding.

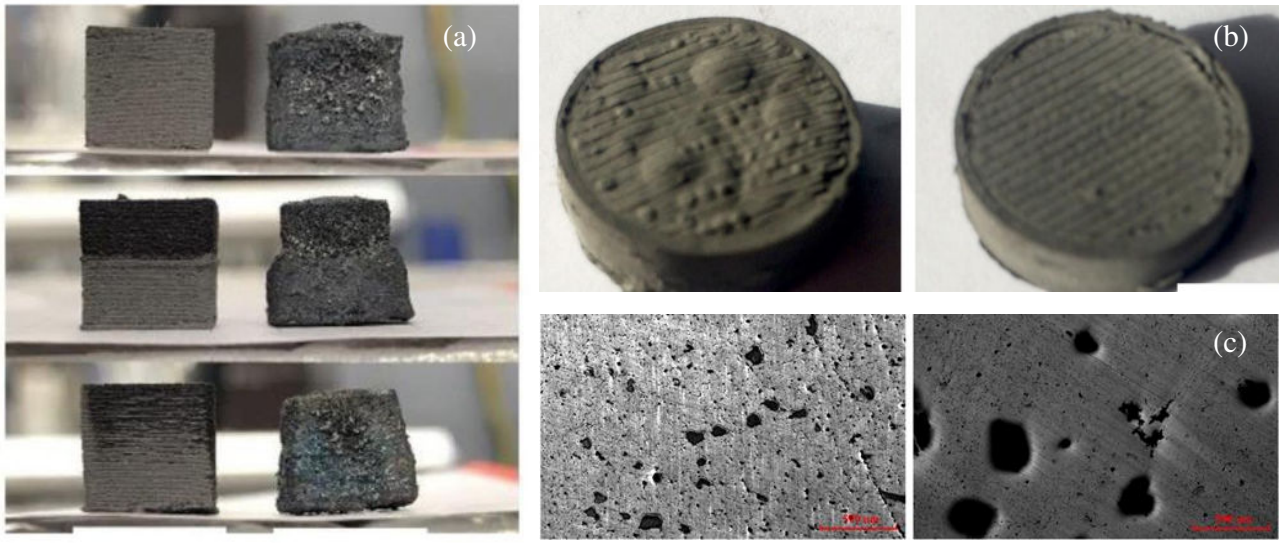

Figure 11: Examples of defects from debinding or sintering due to debinding problems. (a) Distortion [92], (b) blistering and cracking [11], and (c) inconsistent porosity [37]. Panels (a) and (c) reproduced under the terms of a CC-BY license. Panel (b) © Elsevier B.V., reproduced with permission.

6. Discussion on Research Questions

The first objective of this review was to collect and record the successful applications of existing debinding methods for PME parts. It was found that thermal, organic solvent, and catalytic debinding have all been used effectively in several studies each to process parts made with PME. In the cases of thermal and organic solvent debinding, a wide variety of different metal and ceramic powders with different binder combinations were all successfully debinded; the materials and binder compositions were limited for the catalytic debinding, but it was able to process the most common material used thus far in the literature. Sections 4.2-4.5 list the different applications used for PME-manufactured parts. In general, there were no surprises during the review, as the debinding methods performed as expected relative to what was already known in the literature and practice regarding PIM and other traditional powder processes. It was noted that water debinding had not been used for PME parts in the reviewed literature, but no technical or logistical reasons were identified that precluded

it from being used; it seems to simply not have been used in the current literature. A number of potential PME binders and established MEAM polymers are water-soluble. Developing and promoting the use of water debinding could be used to expand the use of PME for more users, as it is simple and safe to use. Thermal debinding requires an expensive programmable furnace and organic solvent and catalytic debinding require fume hoods and chemical processing equipment. The use of water as the solvent could offer a safer and simpler option, especially in education and home use in the future. When water is used, a basic ultrasonic cleaner could be a good tool to help ensure good binder removal before sintering or other processing.

Most of the reviewed papers on debinding of PME did not provide enough discussion and details regarding the basic debinding processes to use them to guide a technical discussion. This is to be expected, as the focus of these studies was on the development of PME methods and materials. In order to fully and properly describe the debinding methods, it was necessary to use references related to binder formation, PIM, and debinding applied to other types of formed powder parts with thermoplastic binders. The main technical discussions in Sections 4.2-4.5 rely on these references. There is a very clear link between the established methods described in the referenced papers and the methods used for the actual PME studies; in most cases, the authors of the PME papers explicitly stated that their debinding methods were based on the traditional methods or cited the older papers describing the methods. No cases were observed where a PME study used a new or modified debinding method, so it can be assumed that the classic debinding methods (including water debinding) are fully useful for PME applications.

Based on the collected literature, the methods used could be easily and fully described and compared with each other. In Section 5, the advantages and disadvantages of each were directly comparable. In addition the pros-cons table (shown in Table 8), this information could also be used to generate a stoplight chart (Table 9) and a comparison of powder percentage value appropriate for each of the debinding methods for PME parts (Table 10). Clearly, the decision about which debinding method to use would be based on a number of factors and considerations, as well as the debinding infrastructure available to do the work. In terms of complex equipment and PPE needed to complete the work, the thermal debinding method is the easiest and has the smallest number of major disadvantages; however, it is very slow and can cause thermal damage to parts. Organic solvent debinding is also widely applicable, but requires safety equipment to use and the chemicals used present safety and environmental risks. In addition, using this process to debind parts with high powder density is sometimes not feasible due to the need to get the liquid solvent to penetrate the part well and carry away the binder. Water and catalytic debinding answer some of these issues but are both quite limited in their application due to the chemical reactions involved.

Manufacturing good-quality feedstock seems to be one of the most effective and easy ways to ensure that the PME parts can be debinded and sintered successfully. This is discussed in depth in Section 3 and Section 5. When using PIM and other powder-mold processes, there is a often a chance for any inconsistencies or problems with the feedstock to be worked out during processing; PME has the opposite effect due to the nature of extrusion-based AM. Any errors in feedstock size or consistency or powder-binder distribution will only be amplified by the structured deposition of the material during processing. Therefore, the tolerance on acceptable feedstock quality is much tighter for PME than what would be needed for most other powder-based processes.

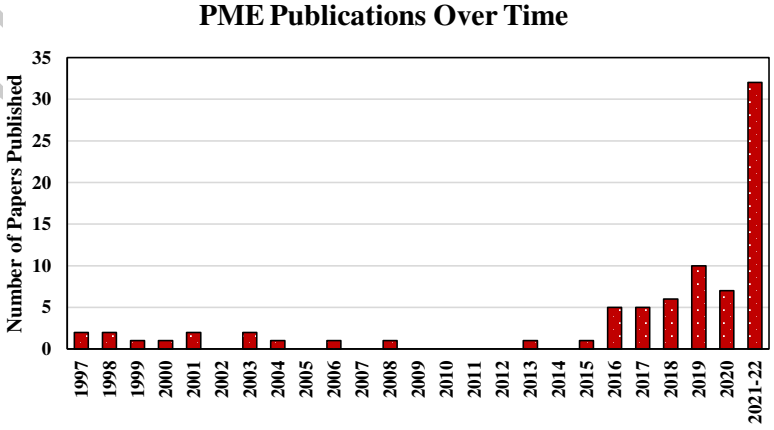

Figure 12: Distribution of publication dates from the reviewed set of references.

Work in the area of PME is clearly a major research topic of recent interest, but it has been something that was proposed in the early days of the MEAM process development. Of the 80 papers collected in this review which explored the PME of green parts and/or the debinding and sintering, 15 of them were published before 2016, the earliest going into print in 1997. Figure 12 shows the distribution of publication dates of the collected papers, tracking the level of interest in this topic over the years. The great amount of recent interest is likely due to a renewed interest in extrusion-based AM processes in general in recent years and the slow-down in the progress of powder-bed metal AM process development. Most of the reviewed papers from this study focused on process development and refinement. There was little to no discussion of design or practical implementation of PME for end-user manufacturing. Therefore, it can be concluded that PME, despite being under discussion of a number of years, is still a developing process and many opportunities remain to be taken.

7. Conclusions and Recommendations for Future Work

This review explored the debinding methods used by and appropriate for use on green parts made using PME. The project started with eight basic research questions, each of which was answered in turn by the collected literature and documented in the sections of this article. After examination and discussion on the collected literature in light of the research questions, eight major conclusions can be drawn.

1. Debinding of PME parts has been shown to be successful for parts based on metal and ceramic powder, as well as mixed powder.
2. Three of the four classic or standard debinding methods have been successfully applied to PME parts and the fourth method is feasible to apply.
3. In terms of debinding procedures, little or no changes need to be made to use the standard processes for PME parts as long as the feedstock is high quality.
4. The quality and construction of the feedstock has a very large effect on the success of the debinding process and must be taken into consideration.
5. The best choice of debinding process for a particular part depends not only on the powder and binder composition, but also the ratio of the powder and binder.
6. For PME parts made from a single powdered material, the thermal debinding process is the easiest and least hazardous to use.
7. PME has a huge amount of future potential, but has not been developed very far yet despite being known since the earliest days of AM development.
8. A large number of the reviewed studies did not give enough technical detail or setup for them to be able to be easily reproduced. As such, there is some uncertainty in the results until more work is done to validate the results. In the meantime, authors should focus on very rigorous presentation of the Materials and Methods sections in their papers to ensure that the results are reproducible.

Nearly all of the papers reviewed focused on the basic process and the materials science behind PME. Three areas where almost no work has been done thus far are related to design, testing methods, and standardization. Future research should focus on these areas, especially in relation to the debinding and sintering processes that happen after printing.

Data Sharing and Availability

Raw data for this article is available upon reasonable request from the corresponding author.

Funding and Acknowledgments

The authors thank the University of Tabriz (Tabriz, Iran) for supporting a portion of this work via a graduate scholarship for Zahra Lotfizarei. The authors also thank the copyright holders of the figures used in this paper for permission to reproduce the figures.

Conflicts of Interest

The authors declare no conflicts of interest. All opinions and conclusions are solely those of the authors and do not necessarily represent the views of their institutions or nor the publisher of the article.

References

[1] Z. Lotfi, A. Mostafapur, and A. Barari, "Properties of metal extrusion additive manufacturing and its application in digital supply chain management," IFAC-PapersOnLine, vol. 54, no. 1, pp. 199–204, 2021.

[2] F. Arbeiter, B. Schrittesser, A. Frank, M. Berer, and G. Pinter, "Cyclic tests on cracked round bars as a quick tool to assess the long term behaviour of thermoplastics and elastomers," Polymer Testing, vol. 45, pp. 83–92, Aug. 2015.

[3] C. Kukla, J. Gonzalez-Gutierrez, I. Duretek, S. Schuschnigg, and C. Holzer, "Effect of particle size on the properties of highly-filled polymers for fused filament fabrication," in AIP Conference Proceedings, AIP, 2017.

[4] P. Singh, V. K. Balla, A. Tofangchi, S. V. Atre, and K. H. Kate, "Printability studies of Ti-6Al-4V by metal fused filament fabrication (MF3)," International Journal of Refractory Metals and Hard Materials, vol. 91, p. 105249, Sept. 2020.

[5] P. Singh, Q. Shaikh, V. K. Balla, S. V. Atre, and K. H. Kate, "Estimating powder-polymer material properties used in design for metal fused filament fabrication (DfMF3)," JOM, vol. 72, pp. 485–495, Nov. 2019.

[6] J. Abel, U. Scheithauer, T. Janics, S. Hampel, S. Cano, A. Müller-Köhn, A. Günther, C. Kukla, and T. Moritz, "Fused filament fabrication (FFF) of metal-ceramic components," Journal of Visualized Experiments, Jan. 2019.

[7] Y. Thompson, J. Gonzalez-Gutierrez, C. Kukla, and P. Felfer, "Fused filament fabrication, debinding and sintering as a low cost additive manufacturing method of 316L stainless steel," Additive Manufacturing, vol. 30, p. 100861, Dec. 2019.

[8] F. Cerejo, D. Gatões, and M. T. Vieira, "Optimization of metallic powder filaments for additive manufacturing extrusion (MEX)," The International Journal of Advanced Manufacturing Technology, vol. 115, pp. 2449–2464, May 2021.

[9] Y. Abe, T. Kurose, M. Santos, Y. Kanaya, A. Ishigami, S. Tanaka, and H. Ito, "Effect of layer directions on internal structures and tensile properties of 17-4ph stainless steel parts fabricated by fused deposition of metals," Materials, vol. 14, p. 243, Jan. 2021.

[10] T. Alkindi, M. Alyammahi, R. A. Susantyoko, and S. Atatreh, "The effect of varying specimens' printing angles to the bed surface on the tensile strength of 3d-printed 17-4ph stainless-steels via metal FFF additive manufacturing," MRS Communications, vol. 11, pp. 310–316, May 2021.

[11] Y. Thompson, M. Polzer, J. Gonzalez-Gutierrez, O. Kasian, J. P. Heckl, V. Dalbauer, C. Kukla, and P. J. Felfer, "Fused filament fabrication-based additive manufacturing of commercially pure titanium," Advanced Engineering Materials, vol. 23, p. 2100380, Sept. 2021.

[12] C. Suwanpreecha and A. Manonukul, "A review on material extrusion additive manufacturing of metal and how it compares with metal injection moulding," Metals, vol. 12, p. 429, Feb. 2022.

[13] J. A. Naranjo, C. Berges, A. Gallego, and G. Herranz, "A novel printable high-speed steel filament: Towards the solution for wear-resistant customized tools by AM alternative," Journal of Materials Research and Technology, vol. 11, pp. 1534–1547, Mar. 2021.

[14] S. Messimer, T. Pereira, A. Patterson, M. Lubna, and F. Drozda, "Full-density fused deposition modeling dimensional error as a function of raster angle and build orientation: Large dataset for eleven materials," Journal of Manufacturing and Materials Processing, vol. 3, p. 6, Jan. 2019.

[15] A. E. Patterson, T. R. Pereira, J. T. Allison, and S. L. Messimer, "IZOD impact properties of full-density fused deposition modeling polymer materials with respect to raster angle and print orientation," Proceedings of the Institution of Mechanical Engineers, Part C: Journal of Mechanical Engineering Science, vol. 235, pp. 1891–1908, Apr. 2019.

[16] B. N. Turner and S. A. Gold, "A review of melt extrusion additive manufacturing processes: II. materials, dimensional accuracy, and surface roughness," Rapid Prototyping Journal, vol. 21, pp. 250–261, Apr. 2015.

[17] "Virtual Foundry." https://thevirtualfoundry.com, 2022. Accessed: 2022-05-21.

[18] "Catamold feedstock for metal injection molding: Processing, properties, and applications," tech. rep., BASF AG, 2003. Accessed 2021-12-05, available online at aerospace.basf.com/catamold.

[19] N. Nestle, M.-C. Hermant, and K. Schmidt, "Mixture for use in a fused filament fabrication process," 2016. Mexico Patent MX2017001014A.

[20] P. Singh, V. K. Balla, A. Gokce, S. V. Atre, and K. H. Kate, "Additive manufacturing of Ti-6Al-4V alloy by metal fused filament fabrication (MF3): producing parts comparable to that of metal injection molding," Progress in Additive Manufacturing, vol. 6, pp. 593–606, Feb. 2021.

[21] C. Kukla, I. Duretek, S. Schuschnigg, J. Gonzalez-Gutierrez, and C. Holzer, "Properties for PIM feedstocks used in fused filament fabrication," in World PM2016 Congress & Exhibition, 9-13 October, 2016, Hamburg, Germany, European Powder Metallurgy Association, 2016.

[22] J. Gonzalez-Gutierrez, S. Cano, S. Schuschnigg, C. Kukla, J. Sapkota, and C. Holzer, "Additive manufacturing of metallic and ceramic components by the material extrusion of highly-filled polymers: A review and future perspectives," Materials, vol. 11, p. 840, May 2018.

[23] C. Lieberwirth, A. Harder, and H. Seitz, "Extrusion based additive manufacturing of metal parts," Journal of Mechanics Engineering and Automation, vol. 7, Feb. 2017.

[24] G. Wu, N. Langrana, S. Rangarajan, R. McCuiston, R. Sadanji, S. Danforth, and A. Safari, "Fabrication of metal components using FDMet: fused deposition of metals," in Proceedings of the 1999 Solid Freeform Fabrication Symposium, August 9-11, 1999, Austin, TX, USA, pp. 11–13, 1999.

[25] N. Cruz, L. Santos, J. Vasco, and F. Barreiros, "Binder system for fused deposition of metals," in Proceedings of the Euro PM2013, Congress & Exhibition, 15-18 September, 2013, Gothenburg, Sweden, 2013.

[26] C. M. Pistor, "Thermal properties of green parts for fused deposition of ceramics (FDC)," Advanced Engineering Materials, vol. 3, pp. 418–423, June 2001.

[27] S. Cano, J. Gonzalez-Gutierrez, J. Sapkota, M. Spoerk, F. Arbeiter, S. Schuschnigg, C. Holzer, and C. Kukla, "Additive manufacturing of zirconia parts by fused filament fabrication and solvent debinding: Selection of binder formulation," Additive Manufacturing, vol. 26, pp. 117–128, Mar. 2019.

[28] M. Carminati, M. Quarto, G. D'Urso, C. Giardini, and G. Maccarini, "Mechanical characterization of AISI 316l samples printed using material extrusion," Applied Sciences, vol. 12, p. 1433, Jan. 2022.

[29] J. Gonzalez-Gutierrez, D. Godec, C. Kukla, T. Schlauf, C. Burkhardt, and C. Holzer, "Shaping, debinding and sintering of steel components via fused filament fabrication," in Proceedings of the 16th International Scientific Conference on Production Engineering, 8-10 June, 2017, Zadar, Croatia, pp. 99–104, 2017.

[30] J. Gonzalez-Gutierrez, F. Arbeiter, T. Schlauf, C. Kukla, and C. Holzer, "Tensile properties of sintered 17-4PH stainless steel fabricated by material extrusion additive manufacturing," Materials Letters, vol. 248, pp. 165–168, Aug. 2019.

[31] H. Gong, D. Snelling, K. Kardel, and A. Carrano, "Comparison of stainless steel 316L parts made by FDM- and SLM-based additive manufacturing processes," JOM, vol. 71, pp. 880–885, Nov. 2018.

[32] C. Lieberwirth, M. Sarhan, and H. Seitz, "Mechanical properties of stainless-steel structures fabricated by composite extrusion modelling," Metals, vol. 8, p. 84, Jan. 2018.

[33] J. Damon, S. Dietrich, S. Gorantla, U. Popp, B. Okolo, and V. Schulze, "Process porosity and mechanical performance of fused filament fabricated 316L stainless steel," Rapid Prototyping Journal, vol. 25, pp. 1319–1327, Aug. 2019.

[34] J. Gonzalez-Gutierrez, D. Godec, R. Guran, M. Spoerk, C. Kukla, and C. Holzer, "3d printing conditions determination for feedstock used in fused filament fabrication (fff) of 17-4ph stainless steel parts," Metalurgija, vol. 57, no. 1-2, pp. 117–120, 2018.

[35] J. Gonzalez-Gutierrez, S. Cano, S. Schuschnigg, C. Holzer, and C. Kukla, "Highly-filled polymers for fused filament fabrication," in Proceedings of the 27th Leoben Polymer Colloquium, 19-20 April, 2018, Leoben, Austria., 2018.

[36] C. Burkhardt, P. Freigassner, O. Weber, P. Imgrund, and S. Hampel, "Fused filament fabrication (FFF) of 316L green parts for the MIM process," in World PM2016 AM - Deposition Technologies, European Powder Metallurgy Association, 2016.

[37] X. Kan, D. Yang, Z. Zhao, and J. Sun, "316l FFF binder development and debinding optimization," Materials Research Express, vol. 8, p. 116515, Nov. 2021.

[38] M. A. Wagner, A. Hadian, T. Sebastian, F. Clemens, T. Schweizer, M. Rodriguez-Arbaizar, E. Carreño-Morelli, and R. Spolenak, "Fused filament fabrication of stainless steel structures - from binder development to sintered properties," Additive Manufacturing, vol. 49, p. 102472, Jan. 2022.

[39] Y. Zhang, S. Bai, M. Riede, E. Garratt, and A. Roch, "A comprehensive study on fused filament fabrication of Ti-6Al-4V structures," Additive Manufacturing, vol. 34, p. 101256, Aug. 2020.

[40] M. Q. Shaikh, P.-Y. Lavertu, K. H. Kate, and S. V. Atre, "Process sensitivity and significant parameters investigation in metal fused filament fabrication of Ti-6Al-4V," Journal of Materials Engineering and Performance, vol. 30, pp. 5118–5134, Apr. 2021.

[41] R. Kumar, N. Ranjan, V. Kumar, R. Kumar, J. S. Chohan, A. Yadav, Piyush, S. Sharma, C. Prakash, S. Singh, and C. Li, "Characterization of friction stir-welded polylactic acid/aluminum composite primed through fused filament fabrication," Journal of Materials Engineering and Performance, vol. 31, pp. 2391–2409, Oct. 2021.

[42] A. F. Sahayaraj, N. S. Kannan, L. Girisha, S. Kannan, D. Rahul, and R. Subbiah, "Performance analysis of peel test on fused filament fabricated polypropylene-aluminium," Materials Today: Proceedings, vol. 47, pp. 5075–5078, 2021.

[43] E. Alberts, M. Ballentine, E. Barnes, and A. Kennedy, "Impact of metal additives on particle emission profiles from a fused filament fabrication 3D printer," Atmospheric Environment, vol. 244, p. 117956, Jan. 2021.

[44] R. Piola, M. Leary, R. Santander, and J. Shimeta, "Antifouling performance of copper-containing fused filament fabrication (FFF) 3-D printing polymer filaments for marine applications," Biofouling, vol. 37, pp. 206–221, Feb. 2021.

[45] J. Gonzalez-Gutierrez, S. Cano, J. V. Ecker, M. Kitzmantel, F. Arbeiter, C. Kukla, and C. Holzer, "Bending properties of lightweight copper specimens with different infill patterns produced by material extrusion additive manufacturing, solvent debinding and sintering," Applied Sciences, vol. 11, p. 7262, Aug. 2021.

[46] Y. Thompson, K. Zissel, A. Förner, J. Gonzalez-Gutierrez, C. Kukla, S. Neumeier, and P. Felfer, "Metal fused filament fabrication of the nickel-base superalloy IN 718," Journal of Materials Science, vol. 57, pp. 9541–9555, Feb. 2022.

[47] M. K. Agarwala, V. R. Jamalabad, N. A. Langrana, A. Safari, P. J. Whalen, and S. C. Danforth, "Structural quality of parts processed by fused deposition," Rapid Prototyping Journal, vol. 2, pp. 4–19, Dec. 1996.

[48] D. Nötzel, R. Eickhoff, and T. Hanemann, "Fused filament fabrication of small ceramic components," Materials, vol. 11, p. 1463, Aug. 2018.

[49] M. Jafari, W. Han, F. Mohammadi, A. Safari, S. Danforth, and N. Langrana, "A novel system for fused deposition of advanced multiple ceramics," Rapid Prototyping Journal, vol. 6, pp. 161–175, Sept. 2000.

[50] R. Atisivan, S. Bose, and A. Bandyopadhyay, "Porous mullite preforms via fused deposition," Journal of the American Ceramic Society, vol. 84, pp. 221–223, Jan. 2001.

[51] A. Bandyopadhyay, K. Das, J. Marusich, and S. Onagoruwa, "Application of fused deposition in controlled microstructure metal-ceramic composites," Rapid Prototyping Journal, vol. 12, pp. 121–128, May 2006.

[52] I. Grida and J. R. Evans, "Extrusion freeforming of ceramics through fine nozzles," Journal of the European Ceramic Society, vol. 23, pp. 629–635, Apr. 2003.

[53] S. Rangarajan, G. Qi, N. Venkataraman, A. Safari, and S. C. Danforth, "Powder processing, rheology, and mechanical properties of feedstock for fused deposition of Si3N4 ceramics," Journal of the American Ceramic Society, vol. 83, pp. 1663–1669, Dec. 2004.

[54] S. Iyer, J. McIntosh, A. Bandyopadhyay, N. Langrana, A. Safari, S. C. Danforth, R. B. Clancy, C. Gasdaska, and P. J. Whalen, "Microstructural characterization and mechanical properties of Si3N4 formed by fused deposition of ceramics," International Journal of Applied Ceramic Technology, vol. 5, pp. 127–137, Mar. 2008.

[55] J. Torres, J. Cotelo, J. Karl, and A. P. Gordon, "Mechanical property optimization of FDM PLA in shear with multiple objectives," JOM, vol. 67, pp. 1183–1193, Mar. 2015.

[56] M. Waseem, B. Salah, T. Habib, W. Saleem, M. Abas, R. Khan, U. Ghani, and M. U. R. Siddiqi, "Multi-response optimization of tensile creep behavior of PLA 3d printed parts using categorical response surface methodology," Polymers, vol. 12, p. 2962, Dec. 2020.

[57] M.-H. Hsueh, C.-J. Lai, C.-F. Chung, S.-H. Wang, W.-C. Huang, C.-Y. Pan, Y.-S. Zeng, and C.-H. Hsieh, "Effect of printing parameters on the tensile properties of 3d-printed polylactic acid (PLA) based on fused deposition modeling," Polymers, vol. 13, p. 2387, July 2021.

[58] C. Gornik and C. Kukla, "Powder injection moulding 2: New method to detect flaws of high-and medium-pressure PIM feedstocks," in Proceedings of the Euro PM2007, Congress & Exhibition, 15-17 October, 2007, Toulouse, France, European Powder Metallurgy Association, 2013.

[59] B. Mutsuddy and R. Ford, Ceramic Injection Molding. Springer New York, NY, 1994.

[60] C. Kukla, J. Gonzalez-Gutierrez, S. Cano, S. Hampel, C. Burkhardt, T. Moritz, and C. Holzer, "Fused filament fabrication (FFF) of PIM feedstocks," in Congreso Iberoamericano de Pulvimetalurgia, 7-9 June, 2017, Ciudad Real, Spain, 2017.

[61] W. Lengauer, I. Duretek, M. Fürst, V. Schwarz, J. Gonzalez-Gutierrez, S. Schuschnigg, C. Kukla, M. Kitzmantel, E. Neubauer, C. Lieberwirth, and V. Morrison, "Fabrication and properties of extrusion-based 3D-printed hardmetal and cermet components," International Journal of Refractory Metals and Hard Materials, vol. 82, pp. 141–149, Aug. 2019.

[62] C. Kukla, J. Gonzalez-Gutierrez, C. Burkhardt, O. Weber, and C. Holzer, "The production of magnets by FFF-fused filament fabrication," in International Powder Metallurgy Congress and Exhibition, Euro PM2017, 1-5 October 2017, Milan, Italy, 2017.

[63] S. Roshchupkin, A. Kolesov, A. Tarakhovskiy, and I. Tishchenko, "A brief review of main ideas of metal fused filament fabrication," Materials Today: Proceedings, vol. 38, pp. 2063–2067, 2021.

[64] S. Krug, J. R. G. Evans, and J. H. H. ter Maat, "Reaction and transport kinetics for depolymerization within a porous body," AIChE Journal, vol. 48, pp. 1533–1541, July 2002.

[65] J. Gonzlez-Gutirrez, G. Beulke, and I. Emri, "Powder injection molding of metal and ceramic parts," in Some Critical Issues for Injection Molding, InTech, Mar. 2012.

[66] T. McNulty, F. Mohammadi, A. Bandyopadhyay, D. Shanefield, S. Danforth, and A. Safari, "Development of a binder formulation for fused deposition of ceramics," Rapid Prototyping Journal, vol. 4, pp. 144–150, Dec. 1998.

[67] S. Pekin, A. Zangvil, and W. Ellingson, "Binder formulation in EVA-wax system for fused deposition of ceramics," in Proceedings of the 1998 Solid Freeform Fabrication Symposium, August 10-12, 1998, Austin, TX, USA, 1998.

[68] P. Thomas-Vielma, A. Cervera, B. Levenfeld, and A. Várez, "Production of alumina parts by powder injection molding with a binder system based on high density polyethylene," Journal of the European Ceramic Society, vol. 28, pp. 763–771, Jan. 2008.

[69] S. Ahn, S. J. Park, S. Lee, S. V. Atre, and R. M. German, "Effect of powders and binders on material properties and molding parameters in iron and stainless steel powder injection molding process," Powder Technology, vol. 193, pp. 162–169, July 2009.

[70] R. K. Enneti, S. J. Park, R. M. German, and S. V. Atre, "Review: Thermal debinding process in particulate materials processing," Materials and Manufacturing Processes, vol. 27, pp. 103–118, July 2011.

[71] C. Quinard, T. Barriere, and J. Gelin, "Development and property identification of 316l stainless steel feedstock for PIM and μPIM," Powder Technology, vol. 190, pp. 123–128, Mar. 2009.

[72] M. Thornagel, "Simulating flow can help avoid mould mistakes," Metal Powder Report, vol. 65, pp. 26–29, Mar. 2010.

[73] Y. Li, S. Liu, X. Qu, and B. Huang, "Thermal debinding processing of 316L stainless steel powder injection molding compacts," Journal of Materials Processing Technology, vol. 137, pp. 65–69, June 2003.

[74] K. Rane, L. D. Landro, and M. Strano, "Processability of SS 316L powder - binder mixtures for vertical extrusion and deposition on table tests," Powder Technology, vol. 345, pp. 553–562, Mar. 2019.

[75] C. Tosto, J. Tirillò, F. Sarasini, and G. Cicala, "Hybrid metal/polymer filaments for fused filament fabrication (FFF) to print metal parts," Applied Sciences, vol. 11, p. 1444, Feb. 2021.

[76] S. Supriadi, B. Suharno, R. Hidayatullah, G. Maulana, and E. R. Baek, "Thermal debinding process of SS 17-4 PH in metal injection molding process with variation of heating rates, temperatures, and holding times," Solid State Phenomena, vol. 266, pp. 238–244, Oct. 2017.

[77] V. Krauss, A. Oliveira, A. Klein, H. Al-Qureshi, and M. Fredel, "A model for PEG removal from alumina injection moulded parts by solvent debinding," Journal of Materials Processing Technology, vol. 182, pp. 268–273, Feb. 2007.

[78] W.-W. Yang, K.-Y. Yang, M.-C. Wang, and M.-H. Hon, "Solvent debinding mechanism for alumina injection molded compacts with water-soluble binders," Ceramics International, vol. 29, pp. 745–756, Jan. 2003.

[79] J. H. H. T. Maat, J. Ebenhöch, and H.-J. Sterzel, "Fast catalytic debinding of injection moulded parts," in 4th International Symposium on Ceramic Materials and Components for Engines, pp. 544–551, Springer Netherlands, 1992.

[80] H. Xie, J. Jiang, X. Yang, Q. He, Z. Zhou, X. Xu, and L. Zhang, "Theory and practice of rapid and safe thermal debinding in ceramic injection molding," International Journal of Applied Ceramic Technology, vol. 17, pp. 1098–1107, Aug. 2019.

[81] H. Lu, "Preliminary mechanical characterization of the low-cost metal 3d printing," Master's thesis, Tennessee Tech University, 2020. Accessed 2022-05-14, available online at https://www.proquest.com/openview/11af4a9f81828f8831b387089d47ce7b/1?pq-origsite=gscholar&cbl=44156.

[82] M. Trunec and J. Cihlář, "Thermal debinding of injection moulded ceramics," Journal of the European Ceramic Society, vol. 17, pp. 203–209, Jan. 1997.

[83] Z. Lu, K. Zhang, and C. Wang, "Effects of oxidation on the strength of debound SiC parts by powder injection moulding," Powder Technology, vol. 208, pp. 49–53, Mar. 2011.

[84] A. Iizuka, T. Ouchi, and T. H. Okabe, "Development of a new titanium powder sintering process with deoxidation reaction using yttrium metal," Materials Transactions, vol. 61, pp. 758–765, Apr. 2020.

[85] L. Urtekin, I. Uslan, and B. Tuc, "Investigation of properties of powder injection-molded steatites," Journal of Materials Engineering and Performance, vol. 21, pp. 358–365, Apr. 2011.

[86] A. Bandyopadhyay, S. C. Danforth, and A. Safari, "Effects of processing history on thermal debinding," Journal of Materials Science, vol. 35, no. 16, pp. 3983–3988, 2000.

[87] M. Pfaffinger, G. Mitteramskogler, R. Gmeiner, and J. Stampfl, "Thermal debinding of ceramic-filled photopolymers," Materials Science Forum, vol. 825-826, pp. 75–81, July 2015.

[88] M. Agarwala, R. van Weeren, A. Bandyopadhyay, A. Safari, S. Danforth, and W. Priedeman, "Filament feed materials for fused deposition processing of ceramics and metals," in Proceedings of the 1996 Solid Freeform Fabrication Symposium, August 12-14, 1996, Austin, TX, USA, 1996.

[89] M. Agarwala, A. Bandyopadhyay, R. van Weeren, N. Langrana, A. Safari, S. Danforth, V. R. Jamalabad, P. J. Whalen, R. Donaldson, and J. Pollinger, "Fused deposition of ceramics (FDC) for structural silicon nitride components," in Proceedings of the 1996 Solid Freeform Fabrication Symposium, August 12-14, 1996, Austin, TX, USA, 1996.

[90] N. A. Conzelmann, L. Gorjan, F. Sarraf, L. D. Poulikakos, M. N. Partl, C. R. Müller, and F. J. Clemens, "Manufacturing complex al_2o_3 ceramic structures using consumer-grade fused deposition modelling printers," Rapid Prototyping Journal, vol. 26, pp. 1035–1048, Mar. 2020.

[91] T. Kurose, Y. Abe, M. V. A. Santos, Y. Kanaya, A. Ishigami, S. Tanaka, and H. Ito, "Influence of the layer directions on the properties of 316l stainless steel parts fabricated through fused deposition of metals," Materials, vol. 13, p. 2493, May 2020.

[92] M. Mousapour, M. Salmi, L. Klemettinen, and J. Partanen, "Feasibility study of producing multi-metal parts by fused filament fabrication (FFF) technique," Journal of Manufacturing Processes, vol. 67, pp. 438–446, July 2021.

[93] K. Gante Lokesha Renukaradhya, "Metal filament 3D printing of SS316L: Focusing on the printing process," Master's thesis, KTH Royal Institute of Technology, Stockholm, Sweden, 2019. Accessed 2022-05-14, available online at http://kth.diva-portal.org/smash/record.jsf?pid=diva2%3A1352994&dswid=417.

[94] S. Riecker, J. Clouse, T. Studnitzky, O. Anderson, and B. Kieback, "Fused deposition modeling-opportunities for cheap metal am," in World PM2016 Congress & Exhibition, 9-13 October, 2016, Hamburg, Germany, European Powder Metallurgy Association, 2016.

[95] M. Sadaf, M. Bragaglia, and F. Nanni, "A simple route for additive manufacturing of 316l stainless steel via fused filament fabrication," Journal of Manufacturing Processes, vol. 67, pp. 141–150, July 2021.

[96] C. Santos, D. Gatões, F. Cerejo, and M. T. Vieira, "Influence of metallic powder characteristics on extruded feedstock performance for indirect additive manufacturing," Materials, vol. 14, p. 7136, Nov. 2021.

[97] S. M. Terry, "Innovating the fused filament fabrication process metal powder polylactic acid printing," Master's thesis, Tennessee Tech University, 2019. Accessed 2022-05-14, available online at https://www.proquest.com/docview/2311651970?pq-origsite=gscholar&fromopenview=true.

[98] Y. Wang, L. Zhang, X. Li, and Z. Yan, "On hot isostatic pressing sintering of fused filament fabricated 316l stainless steel – evaluation of microstructure, porosity, and tensile properties," Materials Letters, vol. 296, p. 129854, Aug. 2021.

[99] S. J. Park and R. M. German, "Master curves based on time integration of thermal work in particulate materials," International Journal of Materials and Structural Integrity, vol. 1, no. 1/2/3, p. 128, 2007.

[100] H. M. Ng, N. M. Saidi, F. S. Omar, K. Ramesh, S. Ramesh, and S. Bashir, "Thermogravimetric analysis of polymers," in Encyclopedia of Polymer Science and Technology, pp. 1–29, John Wiley & Sons, Inc., Nov. 2018.

[101] M. E. Brown, ed., Introduction to Thermal Analysis. Kluwer Academic Publishers, 2004.

[102] D. Heaney, Handbook of metal injection molding. Woodhead Publishing - Elsevier, 2018.

[103] G. Aggarwal, I. Smid, S. J. Park, and R. M. German, "Development of niobium powder injection molding. part II: Debinding and sintering," International Journal of Refractory Metals and Hard Materials, vol. 25, pp. 226–236, May 2007.

[104] R. German, "Progress in titanium metal powder injection molding," Materials, vol. 6, pp. 3641–3662, Aug. 2013.

[105] S. Park, D. Kim, D. Lin, S. Park, and S. Ahn, "Rheological characterization of powder mixture including a space holder and its application to metal injection molding," Metals, vol. 7, p. 120, Mar. 2017.

[106] M. F. F. A. Hamidi, W. S. W. Harun, N. Z. Khalil, S. A. C. Ghani, and M. Z. Azir, "Study of solvent debinding parameters for metal injection moulded 316L stainless steel," IOP Conference Series: Materials Science and Engineering, vol. 257, p. 012035, Oct. 2017.

[107] M. R. Raza, F. Ahmad, N. Muhamad, A. B. Sulong, M. Omar, M. N. Akhtar, M. Aslam, and I. Sherazi, "Effects of debinding and sintering atmosphere on properties and corrosion resistance of powder injection molded 316 L - stainless steel," Sains Malaysiana, vol. 46, pp. 285–293, Feb. 2017.

[108] J. M. Torralba, J. Hidalgo, and A. J. Morales, "Powder injection moulding: processing of small parts of complex shape," International Journal of Microstructure and Materials Properties, vol. 8, no. 1/2, p. 87, 2013.

[109] S. V. Atre, T. J. Weaver, and R. M. German, "Injection molding of metals and ceramics," in SAE Technical Paper Series, SAE International, Sept. 1998.

[110] W. J. Tseng, D.-M. Liu, and C.-K. Hsu, "Influence of stearic acid on suspension structure and green microstructure of injection-molded zirconia ceramics," Ceramics International, vol. 25, pp. 191–195, Mar. 1999.

[111] H. Jorge, L. Hennetier, A. Correia, and A. Cunha, "Tailoring solvent/thermal debinding 316L stainless steel feedstocks for PIM: An experimental approach," in European Congress and Exhibition on Powder Metallurgy. European PM Conference Proceedings, Euro PM2005, pp. 351–356, The European Powder Metallurgy Association, 2005.

[112] W. Liu, Z. Xie, X. Yang, Y. Wu, C. Jia, T. Bo, and L. Wang, "Surface modification mechanism of stearic acid to zirconia powders induced by ball milling for water-based injection molding," Journal of the American Ceramic Society, vol. 94, pp. 1327–1330, Mar. 2011.

[113] J. Wen, Z. Xie, W. Cao, and X. Yang, "Effects of different backbone binders on the characteristics of zirconia parts using wax-based binder system via ceramic injection molding," Journal of Advanced Ceramics, vol. 5, pp. 321–328, Dec. 2016.

[114] M. H. I. Ibrahim, N. Muhamad, A. B. Sulong, N. H. M. Nor, K. R. Jamaludin, M. R. Harun, Murtadhahadi, F. Chinesta, Y. Chastel, and M. E. Mansori, "Optimization of micro metal injection molding by using grey relational grade," in AIP Conference Proceedings, AIP, 2011.

[115] N. C. Fan, W. C. J. Wei, B. H. Liu, A. B. Wang, and R. C. Luo, "Ceramic feedstocks for additive manufacturing," in 2016 IEEE International Conference on Industrial Technology (ICIT), IEEE, Mar. 2016.

[116] C. Suwanpreecha, P. Seensattayawong, V. Vadhanakovint, and A. Manonukul, "Influence of specimen layout on 17-4ph (AISI 630) alloys fabricated by low-cost additive manufacturing," Metallurgical and Materials Transactions A, vol. 52, pp. 1999–2009, Mar. 2021.

[117] C. Suwanpreecha and A. Manonukul, "On the build orientation effect in as-printed and as-sintered bending properties of 17-4ph alloy fabricated by metal fused filament fabrication," Rapid Prototyping Journal, vol. 28, pp. 1076–1085, Jan. 2022.

[118] J. M. Adames, Characterization of polymetric binders for metal injection molding (MIM) process. PhD thesis, University of Akron, 2007. Accessed 2022-01-14, Available online at https://etd.ohiolink.edu/apexprod/rws_etd/send_file/send?accession=akron1194319407&disposition=inline.

[119] M. Nur Syawanie, W. H. Wan Sharuzi, and I. Mohd Halim Irwan, "Experimental study of solvent debinding on water soluble PEG behavior for water atomised SS 316L compact," in Proceedings of The National Conference for Postgraduate Research (NCON-PGR 2016), 24-25 September 2016 , Universiti Malaysia Pahang (UMP), Pekan, Pahang, pp. 187–192, 2016.

[120] G. Chen, P. Cao, G. Wen, and N. Edmonds, "Debinding behaviour of a water soluble PEG/PMMA binder for ti metal injection moulding," Materials Chemistry and Physics, vol. 139, pp. 557–565, May 2013.

[121] H. I. Bakan, "Injection moulding of alumina with partially water soluble binder system and solvent debinding kinetics," Materials Science and Technology, vol. 23, pp. 787–791, July 2007.

[122] M. D. Hayat, G. Wen, M. F. Zulkifli, and P. Cao, "Effect of PEG molecular weight on rheological properties of ti-MIM feedstocks and water debinding behaviour," Powder Technology, vol. 270, pp. 296–301, Jan. 2015.

[123] D. Auzène and S. Roberjot, "Investigation into water soluble binder systems for powder injection moulding," PIM International, vol. 5, no. 1, pp. 51–54, 2011.

[124] G. Chen, G. Wen, N. Edmonds, and P. Cao, "Water debinding behaviour of water soluble ti-MIM feedstock," Powder Metallurgy, vol. 58, pp. 220–227, Apr. 2015.

[125] J. Hidalgo, C. Abajo, A. Jiménez-Morales, and J. Torralba, "Effect of a binder system on the low-pressure powder injection moulding of water-soluble zircon feedstocks," Journal of the European Ceramic Society, vol. 33, pp. 3185–3194, Dec. 2013.

[126] G. Thavanayagam and J. Swan, "Aqueous debinding of polyvinyl butyral based binder system for titanium metal injection moulding," Powder Technology, vol. 326, pp. 402–410, Feb. 2018.

[127] G. Chen, G. Wen, N. Edmonds, P. Cao, and Y. M. Li, "Debinding kinetics of a water soluble binder system for titanium alloys metal injection moulding," Key Engineering Materials, vol. 520, pp. 174–180, Aug. 2012.

[128] P. Ewart, D. L. Zhang, and S. Ahn, "Removal of the water soluble binder components from titanium and titanium alloy powder compacts produced by MIM," Key Engineering Materials, vol. 520, pp. 181–186, Aug. 2012.

[129] P. Suri, R. P. Koseski, and R. M. German, "Microstructural evolution of injection molded gas- and water-atomized 316l stainless steel powder during sintering," Materials Science and Engineering: A, vol. 402, pp. 341–348, Aug. 2005.

[130] S. Banerjee and C. Joens, "Debinding and sintering of metal injection molding (MIM) components," in Handbook of Metal Injection Molding, pp. 129–171, Elsevier, 2019.

[131] X. quan Liu, Y. min li, J. ling Yue, and F. hua Luo, "Deformation behavior and strength evolution of MIM compacts during thermal debinding," Transactions of Nonferrous Metals Society of China, vol. 18, pp. 278–284, Apr. 2008.

[132] J. Radulovic, "Powder injection moulding technology: Properties, possibilities and starting activities," Scientific Technical Review, vol. 65, no. 2, pp. 20–28, 2015.

[133] Y. Kankawa, M. Atarashi, Y. Akifusa, Y. Kaneko, A. Fusamoto, and H. Ikeda, "Injection molding of SUS316l powder with polyacetal polyethylene polymer-alloy polymer.," Journal of the Japan Society of Powder and Powder Metallurgy, vol. 43, no. 7, pp. 840–845, 1996.

[134] M.-A. Porter, "Effects of binder systems for metal injection molding," Master's thesis, Lulea University of Technology, 2003. Accessed 2022-05-14, available online at http://www.diva-portal.org/smash/get/diva2:1017275/FULLTEXT01.pdf.

[135] I. Ait-Mansour, N. Kretzschmar, S. Chekurov, M. Salmi, and J. Rech, "Design-dependent shrinkage compensation modeling and mechanical property targeting of metal FFF," Progress in Additive Manufacturing, vol. 5, pp. 51–57, Mar. 2020.

[136] M. Á. Caminero, A. Romero, J. M. Chacón, P. J. Núñez, E. García-Plaza, and G. P. Rodríguez, "Additive manufacturing of 316l stainless-steel structures using fused filament fabrication technology: mechanical and geometric properties," Rapid Prototyping Journal, vol. 27, pp. 583–591, Jan. 2021.

[137] D. Jiang and F. Ning, "Additive manufacturing of 316l stainless steel by a printing-debinding-sintering method: Effects of microstructure on fatigue property," Journal of Manufacturing Science and Engineering, vol. 143, Apr. 2021.

[138] D. Jiang and F. Ning, "Anisotropic deformation of 316l stainless steel overhang structures built by material extrusion based additive manufacturing," Additive Manufacturing, vol. 50, p. 102545, Feb. 2022.

[139] B. Liu, Y. Wang, Z. Lin, and T. Zhang, "Creating metal parts by fused deposition modeling and sintering," Materials Letters, vol. 263, p. 127252, Mar. 2020.

[140] M. Quarto, M. Carminati, and G. D'Urso, "Density and shrinkage evaluation of AISI 316l parts printed via FDM process," Materials and Manufacturing Processes, vol. 36, pp. 1535–1543, Apr. 2021.

[141] T. Rosnitschek, A. Seefeldt, B. Alber-Laukant, T. Neumeyer, V. Altstädt, and S. Tremmel, "Correlations of geometry and infill degree of extrusion additively manufactured 316l stainless steel components," Materials, vol. 14, p. 5173, Sept. 2021.

[142] G. Fu, N. Loh, S. Tor, B. Tay, Y. Murakoshi, and R. Maeda, "Injection molding, debinding and sintering of 316l stainless steel microstructures," Applied Physics A, vol. 81, pp. 495–500, Aug. 2005.

[143] I. Chang and Y. Zhao, Advances in powder metallurgy. Woodhead Publishing - Elsevier, 2013.

[144] J. Gonzalez-Gutierrez, P. Oblak, B. von Bernstorff, and I. Emri, "Improving powder injection moulding by modifying binder viscosity through different molecular weight variations," in Proceedings of the 11th Global Conference on Sustainable Manufacturing - Innovative Solutions, 23-25 September, 2013, Berlin, Germany., CIRP, 2013.

Appendix A. Thermogravimetric analysis (TGA)

The heating rate β can be calculated as [100, 101]:

$$\beta = \frac{dT}{dt} \tag{A.1}$$

where dT is the change in temperature and dt is the change in time. The thermal kinetics are described by:

$$\frac{d\alpha}{dt} = \kappa(T) f(a) h(P) \tag{A.2}$$

where T is the temperature, κ is the temperature-dependent rate constant, α is the fracture of change or reaction, and P is the pressure. While pressure can have a significant influence on the kinetic processes, $h(P)$ is commonly neglected or assumed to be a constant, as it would be in equilibrium. This equilibrium occurs when all reactive gas reacting with the part is eliminated by releasing the surplus via solid-gas reaction or by flushing by inert gas. It is assumed that the pressure has no influence on the kinetics; therefore, the speed of the process depends on the relationship between the temperature and fraction of change/reaction:

$$\frac{d\alpha}{dt} \approx \kappa(T) f(\alpha) \tag{A.3}$$

In this equation, $\kappa(T)$ and $f(\alpha)$ show the dependence on rate and reaction, respectively. The conversion α is maintained a fraction of overall loss:

$$\alpha = \frac{m_i - m}{m_i - m_f} \tag{A.4}$$

where m_i and m_f are the initial and final mass or weight of the object being debinded. As such, the values of α can vary from 0 to 1 as the part is finished. Finally, the Arrhenius Equation describes the rate constant:

$$\kappa(T) = Ae^{-E/RT} \tag{A.5}$$

where A is the frequency of the reaction driver, E is the activation energy, R is the universal gas constant, and T is the temperature found using TGA.